Effects of lateral heterogeneity on time-domain processing parameters[a]

Yanadet Sripanich[1], Sergey Fomel[2], and Alexey Stovas[3]
[1]Formerly Department of Earth Sciences, Utrecht University, the Netherlands; presently, PTT Exploration and Production Public Company Limited, Bangkok, Thailand;
[2]Bureau of Economic Geology, The University of Texas at Austin, Austin, TX, USA;
[3]Department of Geoscience and Petroleum, Norwegian University of Science and Technology, Trondheim, Norway.

ABSTRACT

Time-domain processing of seismic reflection data has always been an important engine that is routinely utilized to produce seismic images and to expeditiously construct subsurface models. The conventional procedure involves analysing parameters related to the derivatives of reflection traveltime with respect to offset including normal moveout (NMO) velocities (second-order derivatives) and quartic coefficients (fourth-order derivatives). In this study, we propose to go beyond the typical assumption of 1-D laterally homogeneous medium when relating those 'processing' parameters to the subsurface medium parameters and take into account the additional influences from lateral heterogeneity including curved interfaces and smoothly variable velocities. We fill in the theoretical gap from previous studies and develop a general framework for such connection in layered anisotropic media. We show that in general, the influences of lateral heterogeneity get accumulated from all layers via a recursive relationship according to the Fermat's principle and can be approximately quantified in terms of the lateral derivatives of the layer interface surfaces and velocities. Based on the same general principle, we show that our approach can also be used to study the lateral heterogeneity effects on diffraction traveltime and its second-order derivative related to time-migration velocity. In this paper, we explicitly specify expressions for NMO and time-migration velocities with the influences from both types of heterogeneity suitable for 2-D data sets and also discuss possible extensions of the proposed theory to 3-D data sets and to parameters related to higher-order traveltime derivatives. Using numerical examples, we demonstrate that the proposed theory can lead to more accurate reflection and diffraction traveltime predictions in comparison with those obtained based on the 1-D assumption. Both the proposed theoretical framework and its numerical testing for forward traveltime computation presented in this study aid in understanding the effects from lateral heterogeneity on time-processing parameters and also serve as an important basis for designing an efficient technique to separate those influences in important processes such as Dix inversion for a more accurate subsurface model in the future.

INTRODUCTION

Moveout analysis plays an important role in seismic processing and subsurface parameter estimation (Yilmaz, 2001). With regard to pure-mode reflections, the two-way moveout traveltimes are commonly expressed as a Taylor expansion around zero offset with only even powers in the offset direction (Taner and Koehler, 1969). The absence of odd powers is due to the source–receiver reciprocity of pure-mode reflections (Pech et al., 2003; Tsvankin, 2012). The second-order and fourth-order traveltime derivatives in the expansion are related to normal moveout (NMO) velocities and quartic coefficients. Their general expressions have been studied previously (Fomel, 1994;

Pech et al., 2003; Pech and Tsvankin, 2004) and are usually written in terms of the one-way traveltime derivatives of a *normal-incidence ray* traveling from the reflector to the surface according to the normal-incidence-point (NIP) theorem (Krey, 1976; Chernjak and Gritsenko, 1979; Hubral and Krey, 1980; Hubral, 1983; Gritsenko, 1984; Fomel and Grechka, 2001).

A common assumption for evaluating the aforementioned one-way traveltime derivatives and relating them to subsurface medium parameters is to consider a 1-D horizontally-layered anisotropic medium. This assumption generally leads to traveltime and offset being functions of only horizontal phase slownesses (ray parmeters) and allows the traveltime derivatives to be evaluated explicitly, providing a direct bridge between both quantities (e.g, Sripanich and Fomel, 2016; Koren and Ravve, 2017). Despite being strictly applicable to 1-D lateral homogeneous media, this simple connection is normally used to test the accuracy of new moveout approximations in multi-layered media and to relate the estimated (effective) parameters in practice to contributions from different layer (interval) parameters based on Dix-type inversions (e.g, Koren and Ravve, 2006; Ursin and Stovas, 2006; Fomel and Stovas, 2010; Buland et al., 2011; Tsvankin, 2012; Thomsen, 2014).

Seeking to understand and quantify the first-order effects from lateral heterogeneity, Blias (1981) studied the second-order traveltime derivative in a 2-D medium with curved reflectors and variable velocities based on perturbations from 1-D isotropic medium. The result was used to analyze the effects of overburden velocity anomalies on stacking velocities (Blias and Gritsenko, 2003; Blias, 2006, 2009b) and led to a traveltime inversion approach, which honored the effects of lateral heterogeneity (Blias and Khatchatran, 2003). Several other developments along the same line exist in the Russian literature (e.g, Blyas et al., 1984; Gritsenko and Chernjak, 2001) and they were recently reviewed in Russian by Gritsenko (2013). These methods, however, remain applicable only to the case of multi-layered isotropic media.

Assuming that the slowness (1/velocity) varies slowly in the midpoint direction and can be approximated as a Taylor series, Lynn and Claerbout (1982) studied the second-order traveltime derivative in a single horizontal isotropic layer with laterally varying velocity. A similar idea was used by Grechka and Tsvankin (1999) on the group slowness to study the second-order traveltime derivative in one- and two-layered anisotropic models with laterally varying medium parameters. Takanashi and Tsvankin (2011) and Takanashi and Tsvankin (2012) extended the results of Grechka and Tsvankin (1999) to multi-layer anisotropic models with horizontal boundary interfaces (except at the target reflector) and proposed a correction algorithm for removing the effects of embedded velocity anomalies from reflection data. However, the effects from curved reflectors at intermediate interfaces are not considered in these methods.

Apart from moveout analysis, it is also important to note that there is another time-domain processing technique whose governing parameters can be related to one-way traveltime derivatives of some special ray—namely time migration. While moveout analysis relies on its connection to the one-way traveltime derivatives of the normal-incidence ray, time migration relies on its connection to the one-way travel-

time derivatives of the *image ray* (Hubral, 1977). The former denotes the ray that has zero phase slownesses tangent to the reflector, whereas the latter denotes the ray the has zero phase slownesses tangent to the recording surface (Figure 1). For the image ray, the second-order derivative of the one-way (upward) traveltime is related to time-migration velocity, which serves as the basis for time-domain imaging (i.e, collecting contributions along the corresponding diffraction traveltime curve) and also for studying diffraction imaging (Fomel et al., 2007; Reshef and Landa, 2009). Both normal-incidence and image rays may also coincide in some special cases, for example, in a horizontal anisotropic layer with horizontal symmetry plane such as a transversely isotropic medium with vertical symmetry axis (VTI), an orthorhombic medium (ORT), and a monoclinic medium, where both rays become vertical. We note that several researchers have previously studied the process of time migration when underlying velocity models are 'weakly' laterally heterogeneous and some developments were reviewed by Cameron et al. (2007), Schleicher et al. (2007) and Iversen et al. (2012). However, in this study, we shall present an alternative approach to this problem based on an integrated use of Fermat's principle and approximate lateral hetergogeneity effects.
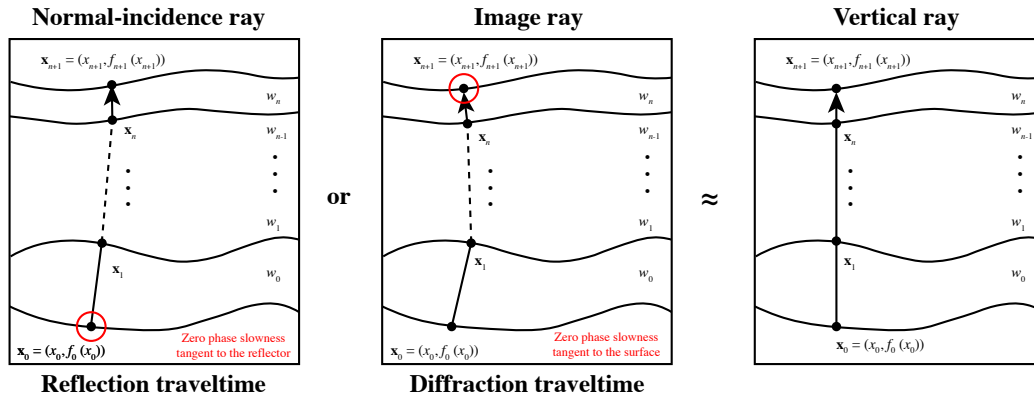

Figure 1: The ray configuration as the basis for computing the traveltime derivatives. We use the vertical ray in a 1-D anisotropic medium at the $\mathbf{x}_0$ location as the reference for the normal-incidence ray and the image ray in the cases of reflection and diffraction traveltimes, respectively.

The fundamental dependency of time-domain processing techniques on the one-way traveltime derivatives of both the normal-incidence ray and the image ray encourages a thorough study on their behaviors under influences from lateral heterogeneity. In this paper, we focus on the *forward* problem and propose a general unified framework for computing one-way traveltime derivatives in the presence of 'weak' lateral heterogeneity from both curved interfaces and smoothly variable medium parameters in a multi-layered anisotropic medium. We rely on the fundamental ideas from Blias (1981), Lynn and Claerbout (1982), and Blyas et al. (1984) to extend the theory to work with perturbations from background 1-D anisotropic medium and demonstrate its connections to existing theories. Particularly, qe show that the effects from lateral heterogeneity in each anisotropic sublayer can be approximately quantified by the

Taylor expansions of interface surfaces and layer group velocities with respect to the 1-D background. Their cumulative effect along the (normal-incidence or image) ray path can then be computed using an exact recursion derived from the Fermat's principle instead of an approximate summation previously used. We test our proposed theory by demonstrating improvements in reflection and diffraction traveltime predictions. In view of these results, we discuss potential applications of this theoretical study such as improving Dix inversion to honor the effects from lateral heterogeneity when inverting for interval parameters.

TRAVELTIME IN GENERAL 2-D LAYERED MEDIA

We consider a 2-D multi-layer model, where the total one-way traveltime from the fixed source $\mathbf{x}_0 = \big(x_0, f_0(x_0)\big)$ on the interface f_0 to the receiver $\mathbf{x}_{n+1} = \big(x_{n+1}, f_{n+1}(x_{n+1})\big)$ on the interface f_{n+1} can be written as

$$t(\mathbf{x}_0, \mathbf{x}_{n+1}) = t_0\big(\mathbf{x}_0, \mathbf{x}_1(h)\big) + \sum_{k=1}^{n} t_k\big(\mathbf{x}_k(h), \mathbf{x}_{k+1}(h)\big) \ , \tag{1}$$

where n is the number of interfaces and $\mathbf{x}_k$ for $k = 1, 2, \ldots, n$ denotes the point of intersection between the ray and the k-th interface (Figure 1). Every intersection point $\mathbf{x}_k$ and the receiver $\mathbf{x}_{n+1}$ depend on the distance $h = x_{n+1} - x_0$, whereas the source at $\mathbf{x}_0$ does not. The two-point traveltime t_k in the k-th layer is given by

$$t_k(\mathbf{x}_k, \mathbf{x}_{k+1}) = \int_{\mathbf{x}_k}^{\mathbf{x}_{k+1}} w_k(\sigma_k) d\sigma_k \ , \tag{2}$$

where σ denotes the arc length along the ray between $\mathbf{x}_k$ and $\mathbf{x}_{k+1}$, and w_k denotes the group slowness (1/group velocity) of the k-th layer that depends on σ_k. Assuming that in each layer w_k only varies horizontally, equation 2 can be rewritten as

$$t_k(\mathbf{x}_k, \mathbf{x}_{k+1}) = \int_{x_k}^{x_{k+1}} \frac{w_k(m_k)}{\sin \theta_k(m_k)} dm_k \ , \tag{3}$$

where m_k denotes the horizontal coordinate (midpoint direction) and θ_k is the angle of the raypath with respect to the vertical. In the following derivation, we assume that the lateral heterogeneity influences are weak and the resulting traveltime perturbations can be computed with respect to a straight raypath in each homogeneous sublayer. Therefore, we assume that θ_k is constant for each k-th layer and rewrite equation 3 as follows (Lynn and Claerbout, 1982; Grechka and Tsvankin, 1999):

$$t_k(\mathbf{x}_k, \mathbf{x}_{k+1}) = \left(\frac{\sqrt{(x_{k+1} - x_k)^2 + (f_{k+1}(x_{k+1}) - f_k(x_k))^2}}{x_{k+1} - x_k} \right) \int_{x_k}^{x_{k+1}} w_k(m_k) dm_k \ . \tag{4}$$

Equations 1 and 4 serve as the basis for our construction in this study, where we seek the following second-order total one-way traveltime derivative,

$$\left. \frac{\partial^2 t}{\partial h^2} \right|_{h=0}, \quad \text{where} \ \ h = x_{n+1} - x_0, \tag{5}$$

evaluated at $h = 0$ with respect to the reference vertical ray in a 1-D anisotropic medium (Figure 1). We denote the reference intersection point by $X = x_0$ and use 'capital letters' to denote quantities evaluated with respect to the reference 1-D anisotropic medium.

In consideration of reflection traveltime, equation 5 is related to the NMO velocity as follows:

$$\frac{1}{V_{nmo}^2} = T \left. \frac{\partial^2 t}{\partial h^2} \right|_{h=0} ,$$

(6)

where T is the one-way zero-offset traveltime from the point $\mathbf{x_0}$ on the reflector to the surface. In the case of diffraction traveltime, equation 5 can be related to time-migration velocity as follows:

$$\frac{1}{V_m^2} = \hat{T} \left. \frac{\partial^2 t}{\partial \hat{x}^2} \right|_{\hat{x}=0} ,$$

(7)

where $\hat{T}$ is the one-way vertical traveltime from the point scatterer $\mathbf{x_0}$ to the surface and we replace h with $\hat{x} = x_{n+1} - x_0$. Even though h and $\hat{x}$ have the same mathematical expression, they represent two different quantities. In case of reflection traveltime, it is common to use h to denote half-offset. On the other hand, in consideration of diffraction traveltime, we use $\hat{x}$ here to denote the distance between the escape location x_0 of image ray and any surrounding point x on the surface. We give a brief review on the derivation of equations 6 and 7 in Appendix A.

Because both NMO velocity (equation 6) for reflection traveltime and time-migration velocity (equation 7) for diffraction traveltime are related to the one-way traveltime derivative of a ray (either normal-incidence or image ray), it is, in principle, sufficient to study the effects from lateral heterogeneity on such derivative of a generic ray travelling between a subsurface position and the surface. We shall adopt this notion in this paper and begin our study by first looking at how the desired second-order one-way traveltime derivative evaluated at the surface (equation 5) is related to the derivatives of t_k in each sublayer based on the Fermat's principle. This relationship will be used to accumulate the total effects of lateral heterogeneity from all sublayers.

A recursive formula from Fermat's principle

To understand how the contribution from each sublayer influences the desired second-order traveltime derivative at the surface, we follow the notion of Blias (1981), Blyas et al. (1984), Gritsenko (1984), and Goldin (1986) and establish the connections between the second-order traveltime derivatives evaluated at different interfaces using the Fermat's principle, which states that the total traveltime t has to be stationary with respect to x_k for $k = 1, 2, \ldots, n$, leading to

$$\frac{\partial t}{\partial x_k} = 0 .$$

(8)

We begin our derivation by first differentiating equation 1 with respect to h, which gives

$$\frac{\partial t}{\partial h} = \frac{\partial t_n}{\partial h} + \sum_{k=1}^{n} \frac{\partial t}{\partial x_k} \frac{\partial x_k}{\partial h}, \tag{9}$$

where n is the index for the topmost layer. Due to the Fermat's condition in equation 8, we then have

$$\frac{\partial t}{\partial h} = \frac{\partial t_n}{\partial h}. \tag{10}$$

Further differentiating equation 10 with respect to h, we arrive at

$$\frac{\partial^2 t}{\partial h^2} = \frac{\partial^2 t_n}{\partial h^2} + \frac{\partial^2 t_n}{\partial h \partial x_n} \frac{dx_n}{dh}, \tag{11}$$

which can be used to compute the desired second-order traveltime derivative $(\partial^2 t/\partial h^2)$. In Appendix B, we show that by differentiating the Fermat's condition in equation 8, the quantity dx_n/dh in equation 11 can be computed from the following recursive formula:

$$r_k = \left(\frac{dx_k}{dh}\right) \bigg/ \left(\frac{dx_{k+1}}{dh}\right) = -\left(\frac{\partial^2 t_k}{\partial x_k \partial x_{k+1}}\right) \bigg/ \left(r_{k-1}\frac{\partial^2 t_{k-1}}{\partial x_{k-1}\partial x_k} + \frac{\partial^2(t_{k-1}+t_k)}{\partial x_k^2}\right), \tag{12}$$

with $k = 1, \ldots, n$. Note that because $h = x_{n+1} - x_0$ and x_0 is independent of h by definition, $dx_0/dh = 0$ and $dx_{n+1}/dh = 1$, which lead to $r_0 = 0$ and $r_n = dx_n/dh$. Equations 11 and 12 suggest that the desired second-order traveltime derivative at the surface can be computed by collecting the contributions from derivatives on t_k from different sublayers through a recursion. The general results for multi-layer media in equations 11 and 12 represent a direct extension of the original findings for two-layer media by Blias (1981), Blyas et al. (1984), Gritsenko (1984), and Goldin (1986). Previously, only the two-layer version of this recursion was adopted and an approximate summation of contributions rather than a recursion was used. We review this proposition in Appendix C and discuss some connections to the exact recursion studied here.

Equations 11 and 12 represent a framework for computing the desired second-order total one-way traveltime derivative at the surface $(\partial^2 t/\partial h^2)$ from second-order one-way traveltime derivatives corresponding to different sublayers (t_k). In the next section, we introduce lateral heterogeneity effects for interfaces f_k and the group slowness w_k to the traveltime in each sublayer t_k in equation 4. We subsequently compute the derivatives on t_k that include both effects, which can then be used by recursion 12.

TAKING HETEROGENEITY INTO ACCOUNT

Finding the layer traveltime derivatives needed by equation 12 is generally straightforward in the case of 1-D media because both traveltime and offset can be conveniently

expressed as functions of horizontal phase slownesses (Sripanich and Fomel, 2016; Koren and Ravve, 2017). However, in this study, we modify the layer traveltime t_k (equation 4) by adding the two sources of lateral heterogeneity: non-flat reflectors and lateral velocity variations.

Non-flat interfaces

To include weak lateral heterogeneity from curved interfaces, we modify equation 4 and consider a Taylor expansion of f_k with respect to the reference location $X = x_0$ as follows:

$$f_k(x_k) \approx f_k(X) + (x_k - X) \left.\frac{\partial f_k}{\partial x_k}\right|_{x_k=X} + \frac{(x_k - X)^2}{2} \left.\frac{\partial^2 f_k}{\partial x_k^2}\right|_{x_k=X} , \qquad (13)$$

$$\approx F_k + (x_k - X)F_k' + \frac{(x_k - X)^2}{2}F_k'' ,$$

where F_k denotes the vertical depth of the k-th interface evaluated at the reference X. F_k' and F_k'' are its corresponding first- and second-order derivatives evaluated at $x_k = X$.

Laterally varying velocity

Following the approach of Lynn and Claerbout (1982) and Grechka and Tsvankin (1999), we assume that the group slowness in each sublayer only varies laterally and can also be approximated as a Taylor expansion with respect to the reference location $X = x_0$ as follows:

$$w_k(m_k) \approx w_k(X) + (m_k - X) \left.\frac{\partial w_k}{\partial m_k}\right|_{m_k=X} + \frac{(m_k - X)^2}{2} \left.\frac{\partial^2 w_k}{\partial m_k^2}\right|_{m_k=X} , \qquad (14)$$

$$\approx W_k + (m_k - X)W_k' + \frac{(m_k - X)^2}{2}W_k'' ,$$

where W_k denotes the group slowness in the k-th layer evaluated at the reference X. In the case of anisotropic media, equation 14 implies the spatial variation of the vertical group slowness with respect to the horizontal coordinate m_k, which follows from the choice of vertical reference ray in the reference 1-D anisotropic medium.

LAYER TRAVELTIME DERIVATIVES WITH HETEROGENEITY

Incorporating the two sources of heterogeneity (equations 13 and 14) into equation 4 and evaluating the integral, we can derive the traveltime t_k that includes the heterogeneity effects. Twice differentiating the result with respect to x_k and x_{k+1} and

evaluating at the vertical reference ($x_k = X$ and $h = 0$), we arrive at the following layer traveltime derivatives:

$$\frac{\partial^2 t_{k-1}}{\partial x_{k-1} \partial x_k}\bigg|_{h=0} = \frac{\partial^2 T_{k-1}}{\partial x_{k-1} \partial x_k}\bigg|_{h=0} + H_1 \ , \tag{15}$$

$$\frac{\partial^2 t_{k-1}}{\partial x_k^2}\bigg|_{h=0} = \frac{\partial^2 T_{k-1}}{\partial x_k^2}\bigg|_{h=0} + H_2 \ ,$$

$$\frac{\partial^2 t_k}{\partial x_k^2}\bigg|_{h=0} = \frac{\partial^2 T_k}{\partial x_k^2}\bigg|_{h=0} + H_3 \ ,$$

where T_k denotes the traveltime of the k-th layer in the reference 1-D horizontally-layered anisotropic media with constant elastic parameters within each layer. Therefore, the terms with T_k derivatives are the usual results ones get under the 1-D medium assumption. The additional heterogeneous terms (H_i) that combine the effects from curved interfaces and laterally varying velocity are given by

$$H_1 = \frac{(F'_{k-1} - F'_k)W'_{k-1}}{2} + \frac{(F_{k-1} - F_k)W''_{k-1}}{6} \ , \tag{16}$$

$$H_2 = -F''_k W_{k-1} - F'_k W'_{k-1} + \frac{(F_{k-1} - F_k)W''_{k-1}}{3} \ ,$$

$$H_3 = F''_k W_k + F'_k W'_k + \frac{(F_k - F_{k+1})W''_k}{3} \ .$$

The expression for $\frac{\partial^2 t_k}{\partial x_k \partial x_{k+1}}$ is similar to that of $\frac{\partial^2 t_{k-1}}{\partial x_{k-1} \partial x_k}$ with shifted indices. If a single horizontal layer is considered, equation 11 becomes reminiscent of the result by Grechka and Tsvankin (1999):

$$\frac{\partial^2 t_0}{\partial h^2}\bigg|_{h=0} = \frac{\partial^2 T_0}{\partial h^2}\bigg|_{h=0} + \frac{(F_0 - F_1)W''_0}{3} \ ,$$

$$= \frac{1}{T_0 V_{nmo}^2} + \frac{(F_0 - F_1)W''_0}{3} \ , \tag{17}$$

but with the second derivative on group slowness as opposed to group velocity. V_{nmo} is the usual normal-moveout velocity in the reference 1-D medium, which translates to V_m in the case of diffraction traveltime.

NUMERICAL IMPLEMENTATION

Using the proposed recursion 12 and the layer traveltime derivatives in equation 15, we can summarize the steps to accumulate the effects from lateral heterogeneity along a raypath and evaluate the corresponding traveltime derivatives at the surface as follows:

1. Given a multi-layered medium with known F, W, and their derivatives in all sublayers, we compute the layer traveltime derivatives (equation 15) for a specified CMP location in the case of reflection traveltime or a specified image-ray

escape location in the case of diffraction traveltime. In particular, equation 15 can be rewritten with evaluated reference 1-D traveltime derivatives as follows:

$$\frac{\partial^2 t_{k-1}}{\partial x_{k-1} \partial x_k}\bigg|_{h=0} = -\frac{1}{T_{k-1} V_{nmo,k-1}^2} + \mathrm{H}_1 \ , \tag{18}$$

$$\frac{\partial^2 t_{k-1}}{\partial x_k^2}\bigg|_{h=0} = \frac{1}{T_{k-1} V_{nmo,k-1}^2} + \mathrm{H}_2 \ ,$$

$$\frac{\partial^2 t_k}{\partial x_k^2}\bigg|_{h=0} = \frac{1}{T_k V_{nmo,k}^2} + \mathrm{H}_3 \ ,$$

where $V_{nmo,k}$ is the NMO velocity of the k-th layer at the specified position. This velocity is constant for an isotropic sublayer but is equal to $V_{P0}\sqrt{1 + 2\delta}$ for a VTI sublayer, where V_{P0} is the vertical P-wave velocity and δ is the Thomsen's delta.

2. We substitute the results from step 1 into the recursion 12 starting from $k = 1$ with $r_0 = 0$ and end up with $r_n = dx_n/dh$.

3. We can evaluate the final second-order traveltime derivative at the surface from equation 11 with the layer derivatives of the n-th layer and r_n from step 2.

4. NMO or time-migration velocity can then be found according to equations 6 and 7 by multiplying the the result from step 3 with the total one-way traveltime in the reference 1-D medium $T = \sum_{k=0}^{n} T_k$.

NUMERICAL EXAMPLES

Single-layer media

In our first example, we consider a medium with a single horizontal layer and a constant horizontal velocity gradient according to

$$v(x) = v_0 + g_x(x - x_0) \ , \tag{19}$$

where g_x is the horizontal velocity gradient. In this medium, the two-point traveltime of a ray between the source at (x_0, z_0) and the receiver at (x, z) can be computed analytically from

$$t(x, z) = \frac{1}{g_x}\mathrm{arccosh}\left(1 + \frac{g_x^2 \left[(x - x_0)^2 + (z - z_0)^2\right]}{2v(x)v_0}\right) \ . \tag{20}$$

The exact second-order derivative of traveltime can then be found by twice differentiating equation 20 with respect to $h = x - x_0$.

We randomly generate 10,000 models from uniform distributions defined with the following parameter ranges:

$$
\begin{aligned}
1.6 \ km/s &\leq v_0 \leq 4.0 \ km/s \ , \\
-0.35 \ 1/s &\leq g_x \leq 0.35 \ 1/s \ , \\
0.0 \ 1/s &\leq g_z \leq 0.2 \ 1/s \ , \\
0.5 \ km &\leq z_0 \leq 3.0 \ km \ .
\end{aligned}
\tag{21}
$$

We compare the performance of equation 17 against the 1-D counterpart, which is equal to $1/T_0 V_{nmo}^2 = 1/T_0 v_0^2$. Figure 2 shows a comparison of histograms for the relative errors of both methods with respect to the analytical results. We can observe that the results from the proposed approach (equation 17) as depicted by the orange histogram has higher peaks at low error levels than that of the overlaid blue histogram associated with the results from the 1-D approach. In other words, the proposed approach can lead to a small level of prediction error in a larger proportion of the generated models. The mean, the standard deviation, and the maximum error from the proposed approach are 0.37, 0.95 and 4.28 per cent in comparison with 1.89, 3.53 and 12.78 per cent from the usual 1-D computation. These results suggest a better performance from the proposed approach and corroborate our theoretical findings.
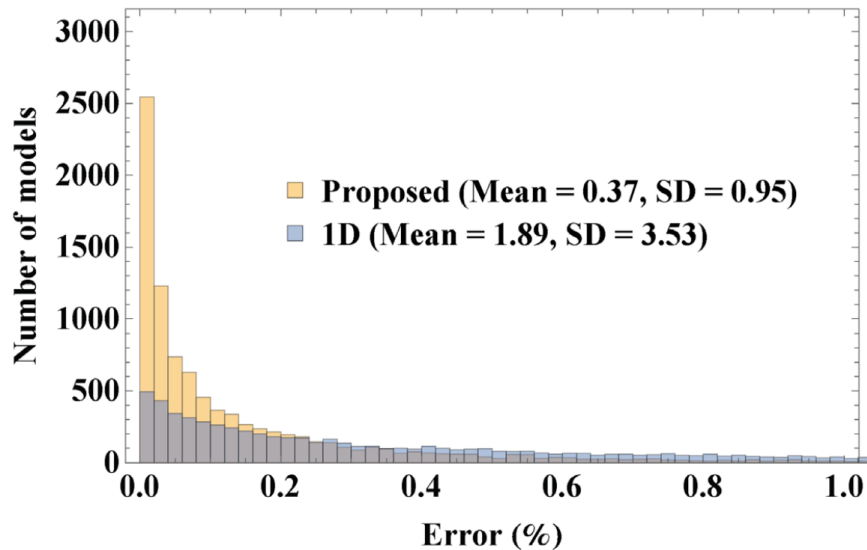

Figure 2: A comparison of error histograms from 10 000 randomly generated models for the results from 1-D computations (Blue) and those from the proposed method (Orange) according to equation 17 in the single layer case with both vertical and horizontal velocity variations. We can observe relatively smaller errors in a larger proportion of the models from the latter, which corroborate our theoretical findings.

For an additional example, we consider a similar setup with only horizontal velocity gradient ($g_x = 0$), which leads to the 1-D traveltime derivative simply being

$1/T_0 V_{nmo}^2 = 1/T_0 v_0^2$. The result of this experiment is shown in Figure 3 with the mean, the standard deviation, and the maximum error from the proposed approach equal to 0.24, 0.48 and 4.28 per cent in comparison with 1.41, 2.45 and 17.58 per cent from the usual 1-D computation. An analogous conclusion to the previous case can be drawn.
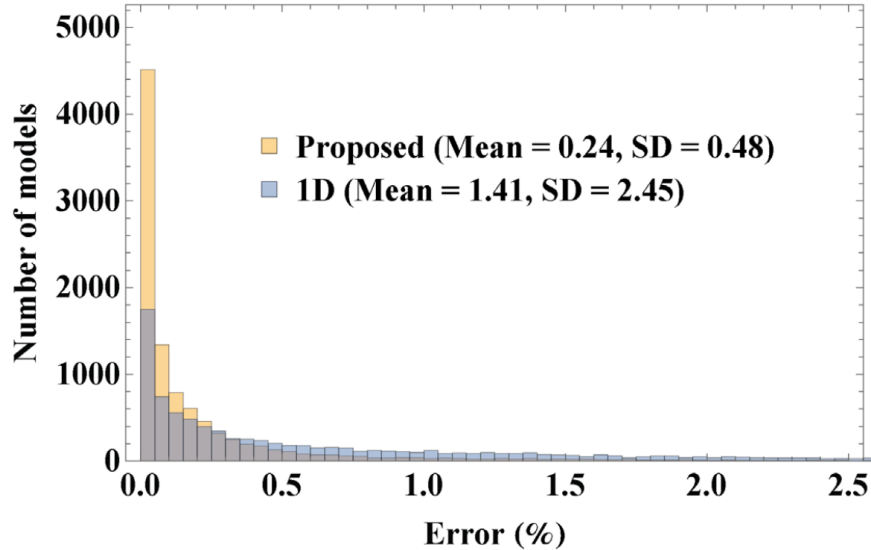

Figure 3: A comparison of error histograms from 10 000 randomly generated models for the results from 1-D computations (Blue) and those from the proposed method (Orange) according to equation 17 in the single layer case with only horizontal velocity variation. We can observe relatively smaller errors in a larger proportion of the models from the latter, which corroborate our theoretical findings.

Reflection traveltime in multilayer media

Next, we consider multi-layered media, where the accumulation of lateral heterogeneity effects with the recursion (equation 12) plays a role. We first look at the case of reflection traveltime and apply the proposed framework to compute the effective NMO velocity that honors the effects from lateral heterogeneity. We follow the steps as described previously in the numerical implementation section. In the first two synthetic examples below, we benchmark our results against synthetic seismograms from Kirchhoff modeling using an accurate two-point ray bending scheme (Sripanich and Fomel, 2014). For the last example, we use the Hess VTI model and its common-midpoint (CMP) gather to demonstrate the applicability of the proposed method.

Layered anisotropic model

We consider first a layered anisotropic model in Figure 4 with parameters shown in Table 1. The model contains both a synclinal structure and a variable dipping layer that can lead to noticeable effects from lateral heterogeneity. Each layer in this model is homogeneous, hence only the effects from curved interfaces (derivatives of F) are important. We note that the depths of the top three reflectors are smaller than 2 km, which is the spread length of offset in this experiment. Therefore, the offset-to-depth ratio is greater than unity and additional effects of moveout nonhyperbolicity caused by anisotropy are important (Tsvankin, 2012). As a result, possible improvement from modifying the NMO velocity proposed under the hyperbolic traveltime assumption in this study may not be as prominent for these three reflectors.
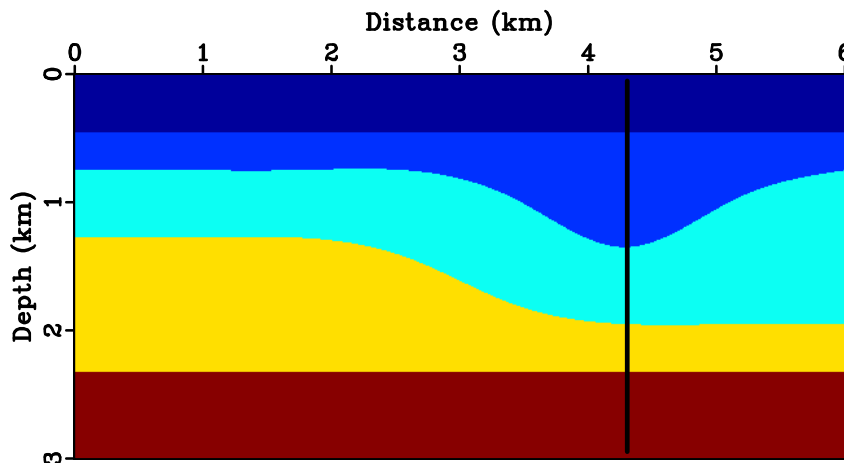

Figure 4: A test subsurface model with a synclinal structure and a variable dipping interface. The solid black line indicates the location of the extracted CMP gather.
aniso/ modcol

Anisotropic parameters	c_{11}	c_{33}	c_{13}	c_{55}	Q_1	Q_3	v_{P0}	v_{S0}	ϵ	δ
Layer 1	9.0	9.0	3.0	3.0	1.0	1.0	3.0	1.732	0.0	0.0
Layer 2	12.72	10.23	5.55	2.57	1.13	1.14	3.20	1.60	0.121	0.046
Layer 3	14.47	9.57	4.51	2.28	1.58	1.68	3.09	1.51	0.256	-0.050
Layer 4	13.0	13.0	5.0	4.0	1.0	1.0	3.61	2.0	0.0	0.0
Layer 5	22.05	14.89	5.34	4.93	1.34	1.423	3.86	2.22	0.240	0.012

Table 1: Anisotropic parameters for the model in Figure 4. The values for layer 2, 4, and 5 are taken from rock samples measurements by Wang (2002), Jones and Wang (1981), and Vernik and Liu (1997), respectively. Q_1 and Q_3 are anelliptic parameters in the Muir-Dellinger scheme convenient for uses in group velocity approximations (Sripanich and Fomel, 2015).

Figure 5 shows the CMP gather at 4.3 km that compares moveout approximations with NMO velocity computed based on the 1-D stratified medium assumption and

from the proposed formula (equation 11). For the bottom two reflectors with the offset-to-depth ratio smaller than unity, we can observe a better performance from the latter with improved flatness of the corrected gather.
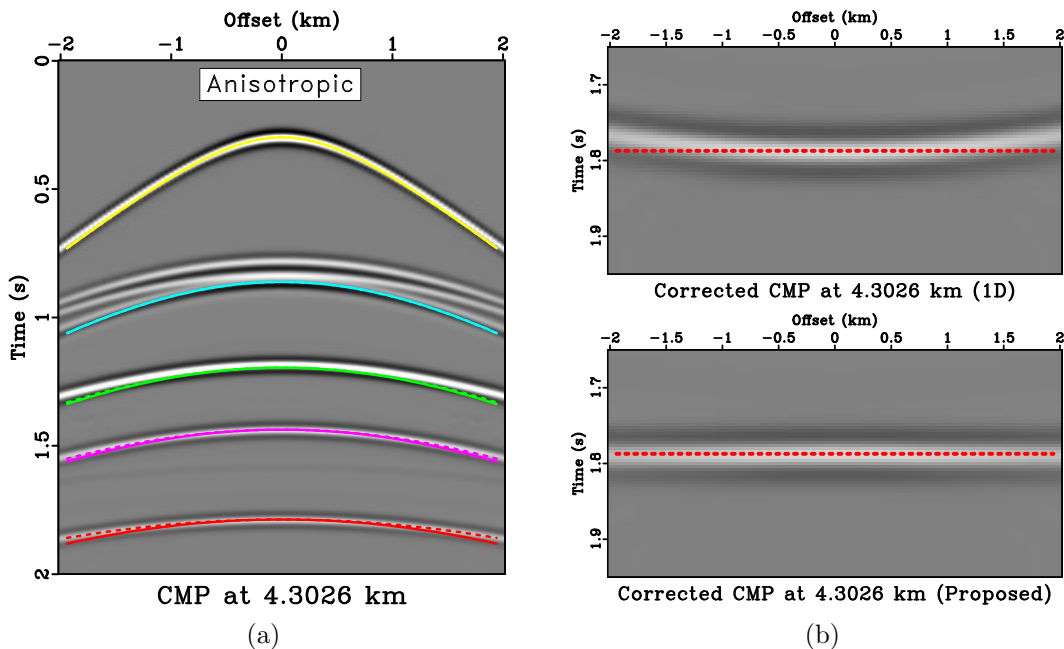

Figure 5: (a) An example CMP gather from the layered anisotropic model at 4.3 *km*. Note the multiple reflection events above the second moveout curve that are caused by the syncline. The solid lines correspond to regular moveout predictions based on the assumption of 1-D stratified model, whereas the dashed lines correspond to those from the proposed framework that takes into account the effects from heterogeneity. (b) Flattened reflections from the bottom interface using the NMO velocity with 1-D assumption (top) and the proposed framework (bottom). We can clearly observe improved flatness from using the proposed framework.

aniso/ hypercompareaniso2,warpedcompareaniso2

Layered isotropic model with velocity gradient

Next, we test the proposed framework in a layered isotropic model with a constant horizontal velocity gradient in each sublayer (equation 19). The model structure is similar to the previous case (Figure 4) and the model parameters are given in Table 2. In this example, both effects from the curved reflectors (derivatives of F) and the laterally varying slowness (derivatives of W) are important. Figure 6 shows the CMP gather at 4.3 *km* that compares the predicted moveout curves based on the 1-D assumption with those from the proposed framework that honor the effects of heterogeneity. We can again observe an improved flatness of moveout-corrected gather from the latter.
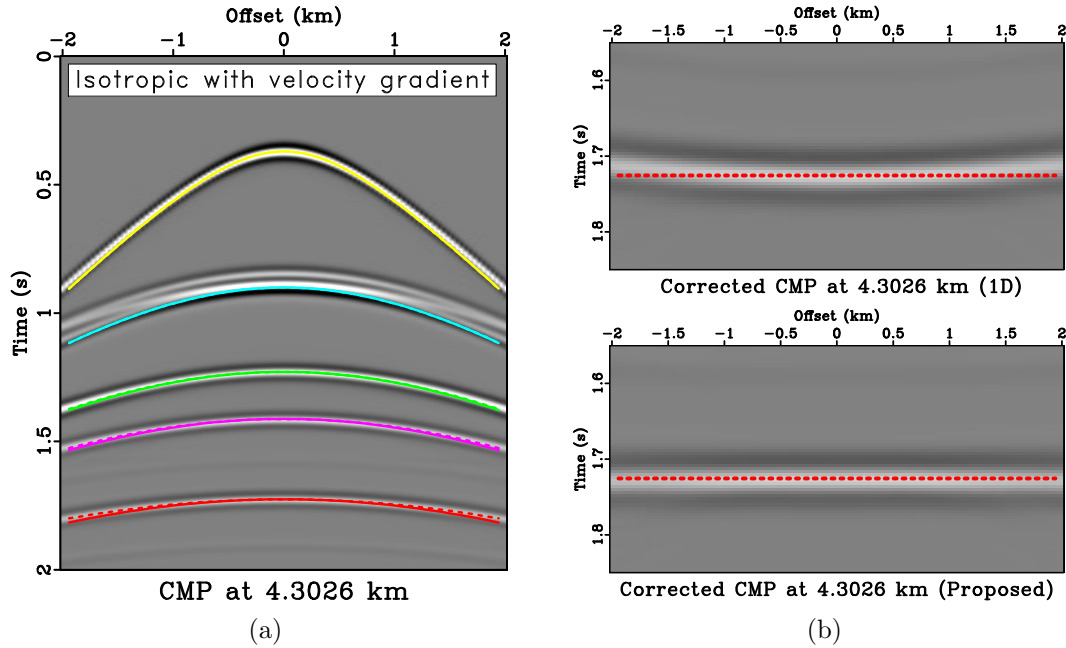
Figure 6: (a) An example CMP gather from the layered isotropic model at 4.3 *km*. Note the multiple reflection events above the second moveout curve that are caused by the syncline. The solid lines correspond to regular moveout predictions based on the assumption of 1-D stratified model, whereas the dashed lines correspond to those from the proposed framework that takes into account the effects from heterogeneity. (b) Flattened reflections from the bottom interface using the NMO velocity with 1-D assumption (top) and the proposed framework (bottom). We can clearly observed improved flatness from using the proposed framework. isograd2/ hypercompare2,warpedcompare2

	v (km/s)	Gradient $(1/s)$
Layer 1	2.50	-0.06
Layer 2	3.20	0.15
Layer 3	3.40	0.20
Layer 4	3.70	0.30
Layer 5	3.86	0.35

Table 2: Model parameters for the layered isotropic model. The reference velocity at 3 *km* and horizontal velocity gradient.

Hess VTI model

For the final example, we consider the Hess VTI model shown in Figure 7 and one of its raw CMP gathers at 11.17 *km*. Due to the well-known limited applicability of time processing in geologically complex media, we only focus at the structure around this CMP gather. This choice allows us to test our approach in a realistic layered anisotropic model, while ensuring that time processing remains applicable. We focus on the effects of curved overburden layers related to the salt structure on reflection traveltime and the corresponding NMO velocity. In this model, the top two layers are isotropic, whereas the third and fourth layers are weakly anisotropic with $\delta = 0.051$ and 0.105, respectively. To ensure an agreement with the condition of offset-to-depth ratio smaller than unity, the offset range up to approximately 2.5 *km* can be considered for the reflection from the bottom of the fourth layer.
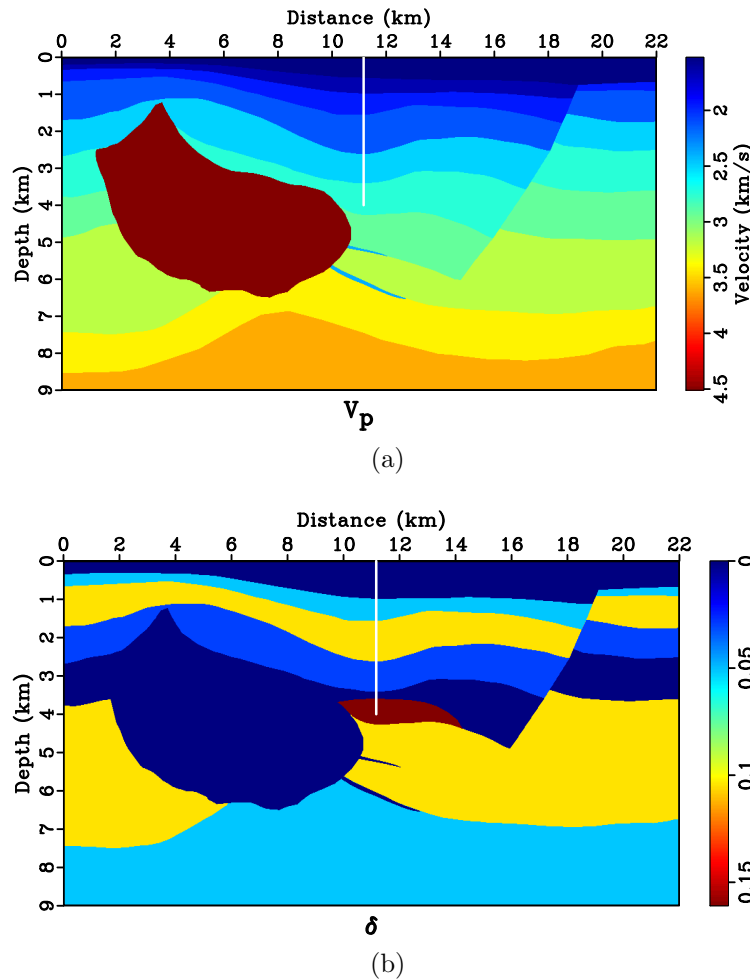

(a)

(b)

Figure 7: (a) Hess VTI model (a) Vertical P-wave velocity and (b) Thomsen's δ with the considered CMP location indicated by the solid white line. hess/ vpline,deltaline

Figure 8 shows the CMP gather up to 4.8 *km* offset range overlain by moveout approximations with NMO velocity computed based on the 1-D stratified medium

assumption and from the proposed formula (equation 11). Focusing on the fourth reflection corresponding to the prominently curved interface, we can observe that the new effective NMO velocity from the proposed method can describe the true reflection traveltime with a higher noticeable accuracy in the range of the offset-to-depth ratio limit (up to 2.5 km). However, even though for this particular reflection from this model, the conclusion seems to also hold beyond 2.5 km offset range, similar observation cannot be made for the third reflection event.
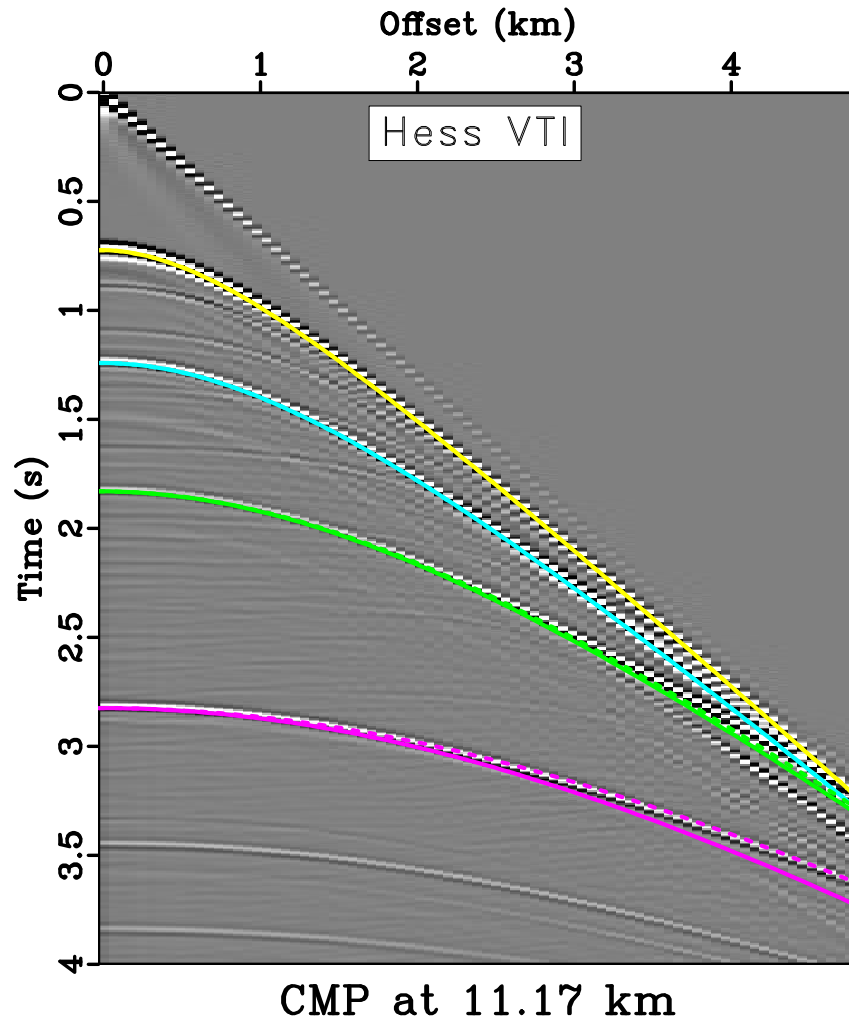

Figure 8: An example raw CMP gather from the Hess VTI model at 11.17 km. The solid lines correspond to regular moveout predictions based on the assumption of 1-D stratified model, whereas the dashed lines correspond to those from the proposed framework that takes into account the effects from heterogeneity. We can observe a better fitting from the latter. hess/ hypercomparehess3

Diffraction traveltime in multilayer media

In this section, we turn our attention to the case of diffraction traveltime and apply the proposed framework to compute the effective time-migration velocity that honors the effects from lateral heterogeneity (equation 7). The synthetic data are generated from Kirchhoff modeling using an accurate two-point ray bending scheme (Sripanich and Fomel, 2014).

Following similar procedure as before, we first evaluate the new expressions of traveltime derivatives in each sublayer above a point diffractor (equation 15) and evaluate the proposed recursive relationship (equations 11 and 12). We finally compute equation 7 using the result from the recursion. We consider the same structural model shown in Figure 4 but replace the bottommost reflector by a point diffractor at 4.3 km.

Layered anisotropic model with a point diffractor

We first consider a similar layered anisotropic model. We limit our consideration of the zero-offset section to a small area around 4.3 km to ensure the validity of the underlying hyperbolic traveltime approximation for time migration. Figure 9a shows the zero-offset section around the point diffractor before time migration with two hyperbolic summation curves generated with migration velocities from the 1-D assumption and from the proposed method. The flattened diffraction travelime hyperbolas with both velocities are shown in Figure 9b, which indicates a better performance of traveltime prediction from the proposed approach. The results from zero-offset Kirchhoff migration is shown in Figure 10 with the focusing comparison shown in Figure 11. We employ a computation of signal envelope to indicate which diffraction responses is better focused. The higher the value of the envelope magnitude at the center, the better focused the response is. The shape of the envelope pattern also qualitatively indicates the degree of symmetry of the distributed energy. We observe a superior diffraction response with higher focusing and more symmetric envelope from the proposed method.

Layered isotropic model with velocity gradient and a point diffractor

In the final example, we consider a similar layered isotropic model with velocity gradient . Again, both effects from the curved reflectors (derivatives of F) and the laterally varying slowness (derivatives of W) are important in this example. To ensure that the image ray is close to the reference vertical ray, we reduce the magnitude of the gradients to 30 % of the original values (Table 2).

Figure 12a shows a zero-offset data around the point diffractor before migration overlain by two hyperbolic summation curves generated with migration velocities from the 1-D assumption and from the proposed method. The corresponding flattened

Figure 9: (a) An example zero-offset section from the layered anisotropic model around 4.3 *km*. The solid lines correspond to regular hyperbolic summation curve based on the assumption of 1-D stratified model, whereas the dashed lines correspond to that from the proposed framework that takes into account the effects from lateral heterogeneity. (b) Flattened diffraction events using the migration velocity with 1-D assumption (top) and the proposed framework (bottom). We can clearly observe improved flatness from using the proposed framework, which indicates a better traveltime prediction and in turn, a more focused migrated response. anisodiffraction/ hypercompareanisodiff3,warpedhypercompareaniso3
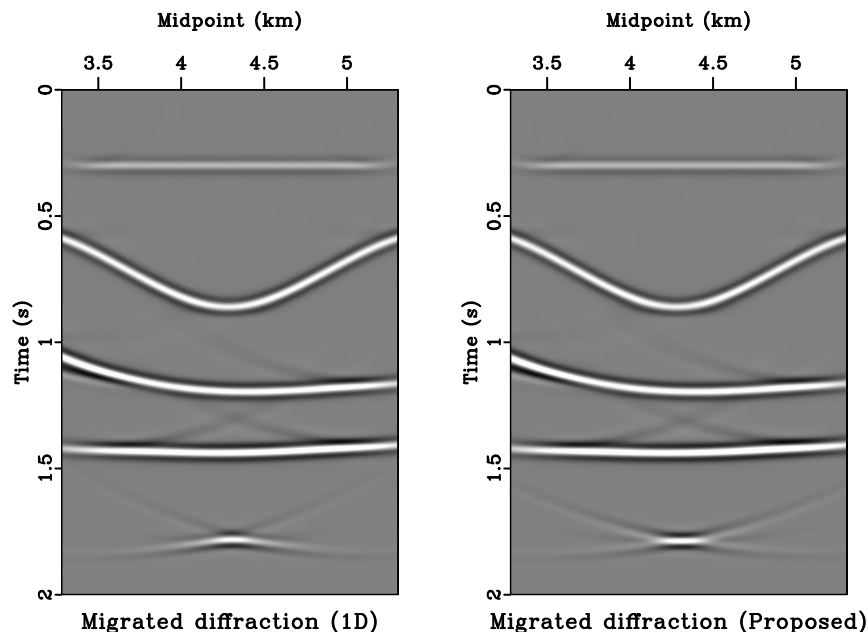
Figure 10: A zero-offset migrated section for the layered anisotropic model. The resultant point diffractor appears to be better focused from the proposed method (right) than from the regular migration velocity based on 1-D assumption (left). anisodiffraction/ migcompareaniso

diffraction travelime hyperbolas are shown in Figure 12b, which suggests a superior performance in traveltime prediction from the proposed method. Figure 13 shows the results from zero-offset Kirchhoff migration and Figure 14 shows their envelope focusing comparison. Similarly to the layered anisotropic case, we observe a superior diffraction response with higher and more symmetric focusing from the proposed method.

DISCUSSION

It is worth emphasizing that even though we rely on the accuracy of traveltime predictions to verify the effectiveness of our proposed framework, it is not intended to be used in place of other numerical methods that can compute the traveltime derivatives more accurately such as the paraxial ray theory. The importance of our work lies in its contribution to the fundamental understanding on how effects from lateral heterogeneity can be characterized (derivatives of F and W) and on how they can affect the parameters—normal-moveout velocity and time-migration velocity—we routinely use in time processing. The relationship between traveltime derivatives at different surfaces that leads to the recursion (equation 12) employed in this study is also closely related to that used in the development of important processing techniques such as Dix inversion. To elaborate on this final point further, we can take, for example, the

Figure 11: A focusing comparison of migrated point diffractors for the layered anisotropic model. The proposed method leads to a higher magnitude of the focusing at the center and a more symmetric response, which indicates its superior performance. anisodiffraction/ envcompareaniso
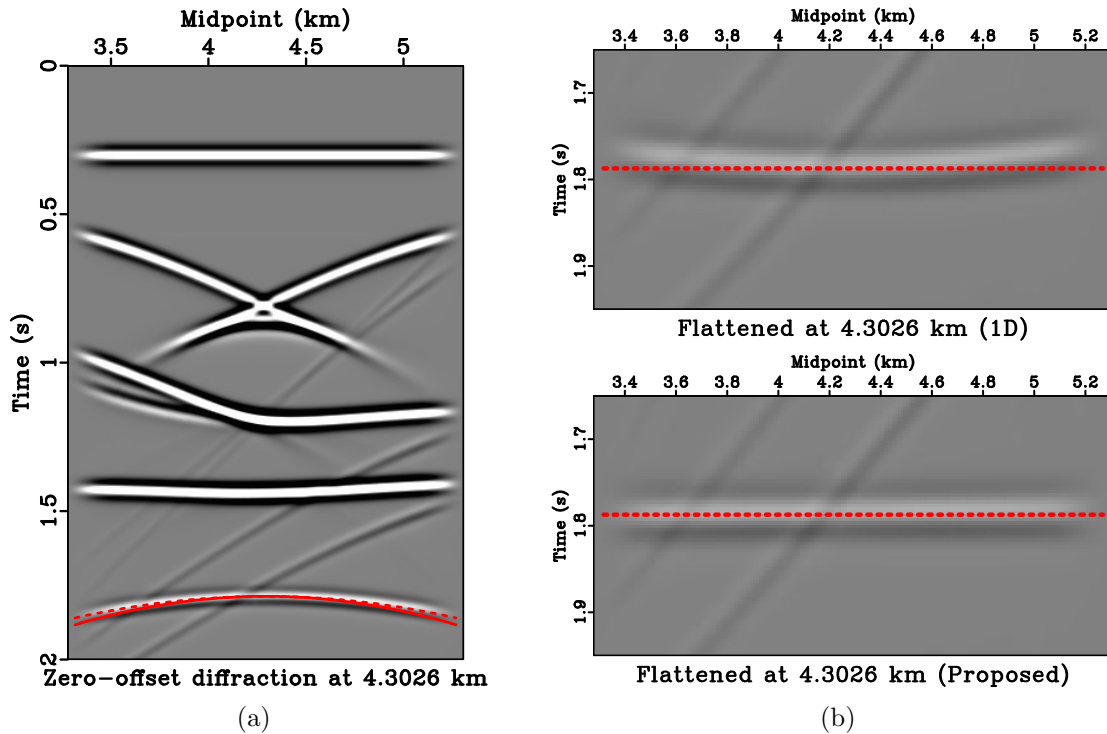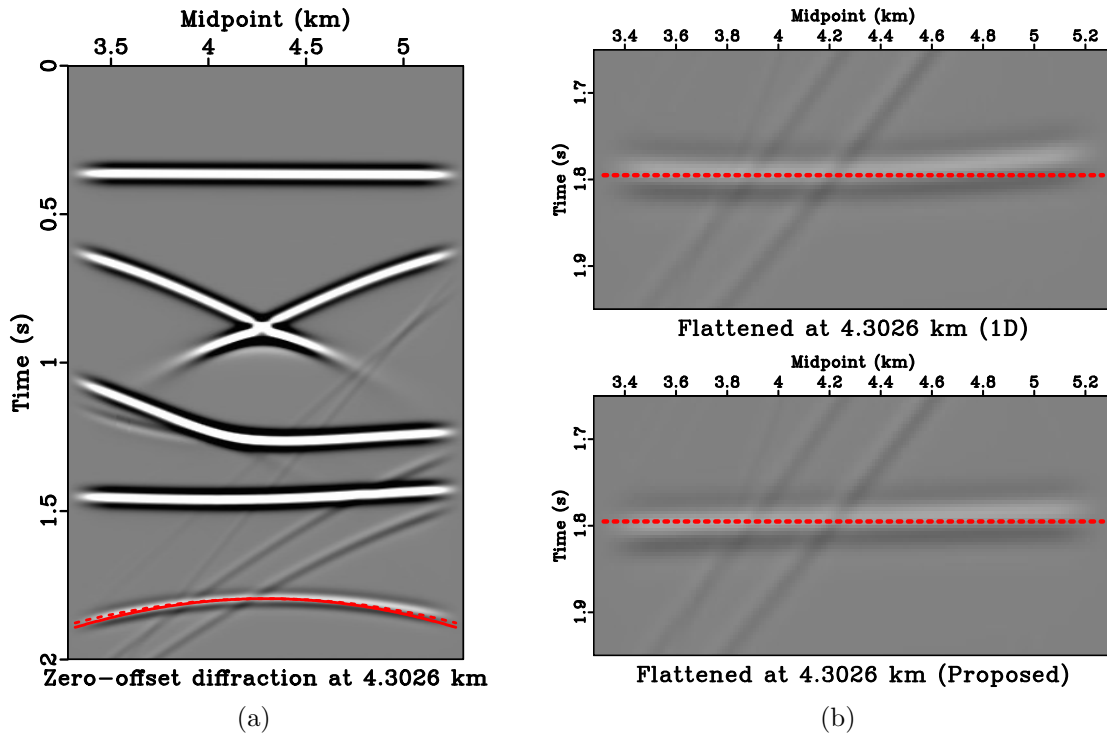
Figure 12: An example zero-offset section from the layered isotropic model around 4.3 *km*. The solid lines correspond to regular hyperbolic summation curve based on the assumption of 1-D stratified model, whereas the dashed lines correspond to that from the proposed framework that takes into account the effects from lateral heterogeneity. (b) Flattened diffraction events using the migration velocity with 1-D assumption (top) and the proposed framework (bottom). We can clearly observe improved flatness from using the proposed framework, which indicates a better traveltime prediction and in turn, a more focused migrated response. diffraction/ hypercomparediff3,warpedhypercompare3
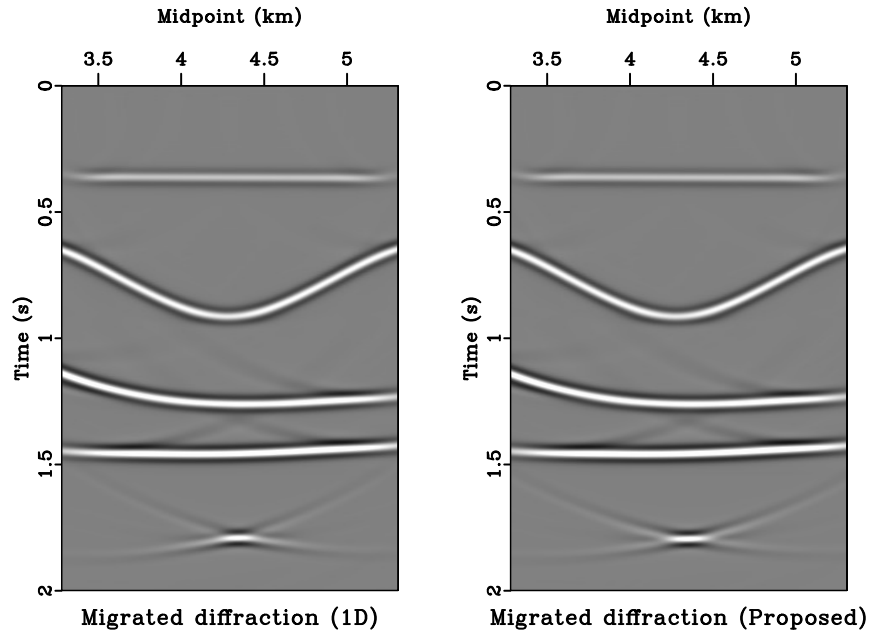
Figure 13: A zero-offset migrated section for the layered isotropic model. The resultant point diffractor appears to be better focused from the proposed method (right) than from the regular migration velocity based on 1-D assumption (left). diffraction/ migcompare

relationship for a two-layered medium given by equation 43,

$$\frac{\partial^2 t}{\partial h^2} = \frac{\partial^2 t_1}{\partial h^2} - \left(\frac{\partial^2 t_1}{\partial x_1 \partial h} \right)^2 \bigg/ \left(\frac{\partial^2 (t_0 + t_1)}{\partial x_1^2} \right) \ . \tag{22}$$

For horizontal homogeneous isotropic sublayers, the pertaining traveltime derivatives can be expressed as

$$\begin{aligned}
\frac{\partial^2 t_1}{\partial h^2} \bigg|_{h=0} &= \frac{1}{D_1/W_1} = \frac{1}{T_1 V_1^2} \ , \\
\frac{\partial^2 t_1}{\partial x_1 \partial h} \bigg|_{h=0} &= -\frac{1}{D_1/W_1} = -\frac{1}{T_1 V_1^2} \ , \\
\frac{\partial^2 t_0}{\partial x_1^2} \bigg|_{h=0} &= \frac{1}{D_0/W_0} = \frac{1}{T_0 V_0^2} \ , \\
\frac{\partial^2 t_1}{\partial x_1^2} \bigg|_{h=0} &= \frac{1}{D_1/W_1} = \frac{1}{T_1 V_1^2} \ ,
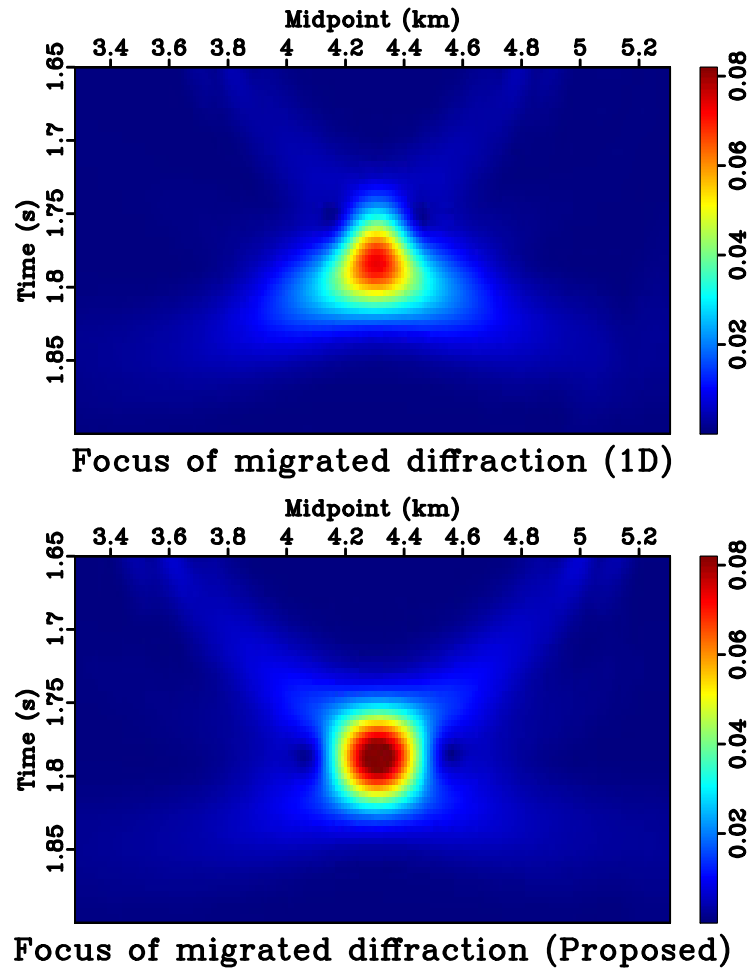\end{aligned} \tag{23}$$
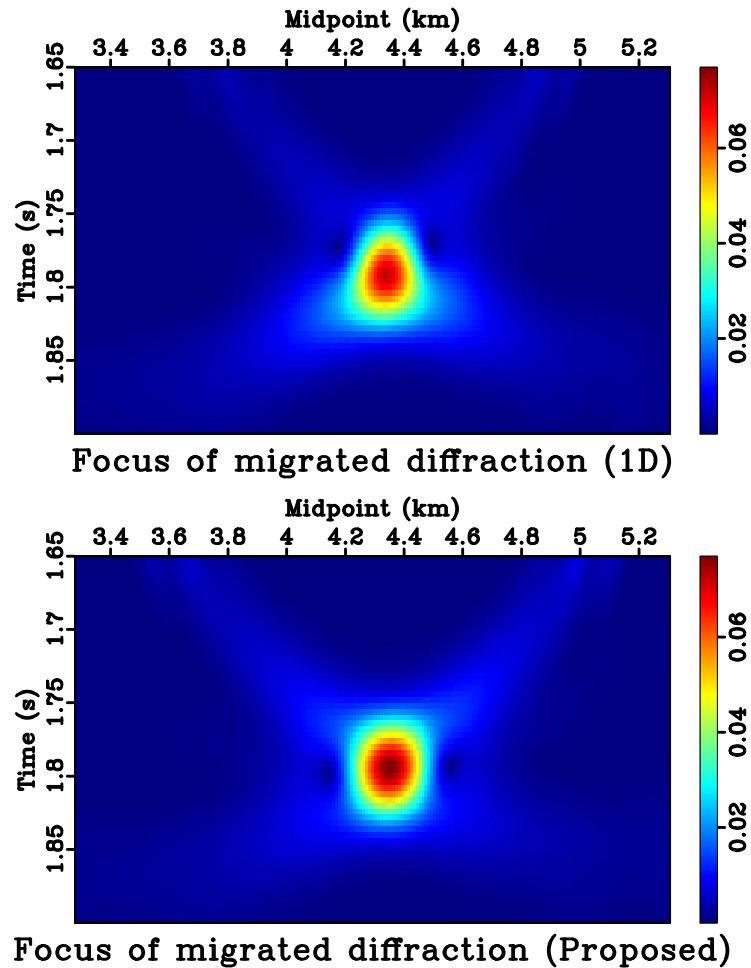
Figure 14: A focusing comparison of migrated point diffractors for the layered isotropic model. The proposed method leads to a higher magnitude of the central focusing at the center and a more symmetric response, which indicates its superior performance. diffraction/ envcompare

where D_k is the thickness of the k-th layer and $V_k = 1/W_k$ denotes its velocity. Substituting equation 23 into equation 22 gives

$$\left.\frac{\partial^2 t}{\partial h^2}\right|_{h=0} = \frac{1}{T_1 V_1^2} - \left(-\frac{1}{T_1 V_1^2}\right)^2 \bigg/ \left(\frac{1}{T_0 V_0^2} + \frac{1}{T_1 V_1^2}\right) ,$$
$$= \frac{1}{T_0 V_0^2 + T_1 V_1^2} , \tag{24}$$

which leads to

$$V_{nmo}^2 = \left[(T_0 + T_1) \left.\frac{\partial^2 t}{\partial h^2}\right|_{h=0}\right]^{-1} ,$$
$$= \frac{T_0 V_0^2 + T_1 V_1^2}{T_0 + T_1} . \tag{25}$$

Equation 25 serves as the basis for computing the effective NMO velocity, which is similar to the root-mean-square (RMS) velocity in this simple case. Dix-type inversion in this example follows directly from equation 25, where one seeks to estimate the velocity at the bottom layer V_0 from a measured V_{nmo} at the surface according to

$$V_0^2 = \frac{(T_0 + T_1)V_{nmo}^2 - T_1 V_1^2}{(T_0 + T_1) - T_1} . \tag{26}$$

Alternative derivations for Dix-type inversion can be done in the phase domain, where the traveltime and offsets are expressed as functions of ray parameters (Tsvankin, 2012; Sripanich and Fomel, 2016; Koren and Ravve, 2017). Future investigations are required to establish a Dix-type inversion approach that honors the effects from lateral heterogeneity based on the result of this work.

Another possible extension of this work is to apply the proposed theory in the context of velocity anomaly removal similar to Blias (2009a), Takanashi and Tsvankin (2011), and Takanashi and Tsvankin (2012). In light of our result on the need of a recursive relationship (equation 12) to collect lateral heterogeneity effects from both curved interfaces and variable medium parameters, it remains to be investigated how the contribution from any individual layer with embedded velocity anomaly can be removed in an accurate and efficient manner.

The proposed method takes into account the effects from lateral heterogeneity by modifying the second-order traveltime derivative related to NMO velocity (reflection) or time-migration velocity (diffraction). Therefore, the limit on the validity of the hyperbolic traveltime assumption in both cases is still enforced. We further discuss the possibility of extending our framework to higher-order traveltime derivatives in Appendix D, where the conventional paraxial ray theory is no longer applicable. A possible 3D extension of the proposed framework is investigated in Appendix E, where we observe that an additional solve of a linear system of equations at each interface surface is needed to track the higher number of pertaining parameters in 3D. However, a direct solve of this system is generally not possible due to a smaller

number of equations than unknowns. This problem was conveniently circumvented in the 2D case due to the smaller number of associated parameter (only one) and the use of a recursive relationship, which is no longer straightforward to formulate in the 3D case. Consequently, further investigations are required to extend the proposed framework to work with 3D datasets.

Our method takes into account the first-order effects from lateral heterogeneity in largely flat subsurface, which ensures that the normal-incidence ray and the image ray stays close to the reference vertical direction. Consequently, our approach does not substitute the dip-moveout process (DMO) for handling effects from dipping reflectors, which becomes prominent as the dip increases. The Gardner continuation (Fomel, 2014) serves as an alternative means to rid the moveout velocity on its dip dependency by transforming the prestack data into a special domain.

In our framework, we choose to consider the traveltime expression in the group domain, where it depends on the medium parameters and the spatial location in Cartesian coordinates. This choice allows for practical convenience when considering information at the zero offset and is appropriate for predominantly horizontally layered media with weak heterogeneity effects such as in land datasets associated with unconventional reservoirs. An alternative formulation can also be constructed in the phase domain, which can be advantageous when considering more complex media with arbitrarily dipping interfaces (Grechka and Tsvankin, 2002; Grechka et al., 2002).

Finally, we note that the results from this study, coupled with accurate moveout functional forms (Fomel and Stovas, 2010; Sripanich et al., 2017), may serve as the basis for possible future improvements of practical moveout inversion techniques that take into account the lateral heterogeneity effects. Subsequent applications of time-to-depth conversion methods that also honor lateral heterogeneity can potentially lead to an improved time-domain imaging workflow and a more accurate subsurface velocity model efficiently obtained from time processing (Cameron et al., 2007; Li and Fomel, 2015; Valente et al., 2017; Sripanich and Fomel, 2018). The latter is especially favorable as it may represent a good starting model for more sophisticated tomographic or full-waveform inversion techniques and lead to better convergence.

CONCLUSIONS

We have proposed a general framework for evaluating the one-way traveltime derivatives in layered anisotropic media in the presence of weak lateral heterogeneity from curved reflectors and lateral velocity variations. Relying on the Fermat's principle, we show that in 2D media, the effects from lateral heterogeneity in each sublayer gets accumulated according to a recursive relationship. We specify the expressions for the second-order traveltime derivatives related to NMO velocity and time-migration velocity suitable for 2D datadets that honor these effects from lateral heterogeneity. We subsequently show that the new expressions can lead to improved moveout pre-

dictions and better focused diffraction responses. The results of this study fill in the missing gap in existing theory and serve as a basis for understanding and quantifying the first-order effects of lateral heterogeneity on reflection and diffraction traveltimes in multi-layer anisotropic media. The fundamentals provided in this work is important for future design of accurate parameter estimation techniques such as Dix-type inversion that honor the effects from lateral heterogeneity.

ACKNOWLEDGMENTS

APPENDIX A
REVIEW OF REFLECTION AND DIFFRACTION TRAVELTIME APPROXIMATIONS

The basis of our construction in this paper is the one-way traveltime in general layered media and its derivatives. In this appendix, we review an important concept on how this one-way traveltime can be related to two-way reflection and diffraction traveltimes, which signifies the importance of the presented results. For simplicity, we only show the expressions in the 2D case.

Reflection traveltime

Reflection traveltimes (moveout) are commonly expressed as a Taylor series of two-way traveltime squared around zero offset with only even powers (Taner and Koehler, 1969). Assuming pure-mode reflections with source-receiver reciprocity and symmetric raypaths between the incident and the reflected waves around zero offset in 1D media, we can construct a two-way reflection traveltime approximation by adding two one-way traveltime approximations (from $-h$ and $+h$) as follows (Thomsen, 2014; Tsvankin, 2012; Sripanich and Fomel, 2016):

$$2t(h) = 2T + h^2 \left(\frac{\partial^2 t}{\partial h^2} \right) \bigg|_{h=0} + \frac{h^4}{12} \left(\frac{\partial^4 t}{\partial h^4} \right) \bigg|_{h=0} + \cdots . \tag{27}$$

We follow the same notation as in the main text and use T to denote one-way zero-offset traveltime. Equation (27) can be converted to a more commonly known series in two-way traveltime squared in terms of full offsets $(2h)$ as follows:

$$4t^2(2h) \approx 4T^2 + a_2(2h)^2 + a_4(2h)^4 , \tag{28}$$

where a_2 and a_4 are coefficients related to the NMO velocity and the quartic coefficient, respectively. Both parameters can be expressed in terms of the derivative of one-way traveltime around zero offset as follows (Al-Dajani and Tsvankin, 1998; Sripanich and Fomel, 2016):

$$a_2 = T \frac{\partial^2 t}{\partial h^2} \bigg|_{h=0} , \tag{29}$$

$$a_4 = \frac{1}{16} \left[\left(\frac{\partial^2 t}{\partial h^2} \right)^2 + \frac{T}{3} \frac{\partial^4 t}{\partial h^4} \right] \bigg|_{h=0} . \tag{30}$$

We emphasize that two important assumptions are made in the derivation so far:

1. We only consider pure-mode reflections with source-receiver reciprocity.

2. The incident and reflected raypaths are symmetric around zero offset.

Except for some special configurations, the first assumption is generally absent in consideration of converted waves and the series of reflection traveltime will also contain terms with odd powers (Tsvankin and Grechka, 2011; Thomsen, 2014; Koren and Ravve, 2017). On the other hand, the second assumption ensures the absence of reflection dispersal, which in turn, suggests that zero offset corresponds to the vertical ray. When this assumption does not hold, the fourth-order reflection traveltime coefficient (a_4) becomes more complex than what is shown in equation (30) (Pech et al., 2003; Koren and Ravve, 2017). Grechka and Tsvankin (1998) emphasized that reflection dispersal has no effect on NMO velocity related to equation (29) (Hubral and Krey, 1980). It becomes important only when considering higher-order traveltime coefficients such as a_4 in equation (30).

In this paper, we only utilize the relationship between the reflection traveltime coefficients (a_2) and the second-order derivative of the one-way traveltime of the fictional normal-incidence ray in equation (29), which is not affected by reflection dispersal. Therefore, NMO velocity can be computed from

$$V_{nmo}^2 = \frac{1}{a_2} \, , \tag{31}$$

as shown in equation (6). However, we emphasize the importance of the aforementioned assumptions and advise careful consideration when extending our framework to study higher-order reflection traveltime coefficients such as a_4.

Diffraction traveltime

As a more fundamental alternative to study seismic responses, one can choose to consider a reflecting point (scatterer) instead of a reflecting surface because any model is a superposition of such scatterers. Assuming that the subsurface velocity v is constant, the total (diffraction) traveltime of the wave traveling in this configuration is simply a sum of traveltime of the two legs, which can be expressed by the double-square-root (DSR) equation (Claerbout, 1996):

$$t_s + t_r = \sqrt{\hat{T}^2 + \left(\frac{m - h - x_0}{v}\right)^2} + \sqrt{\hat{T}^2 + \left(\frac{m + h - x_0}{v}\right)^2} \, , \tag{32}$$

where m denotes midpoint, h denotes half offset, x_0 denotes the horizontal coordinate of the point scatterer, and $\hat{T}$ is a one-way vertical traveltime from the point scatterer to the surface. The true location of the point scatterer x_0 will also be the same as the emerging location of the image rays (Hubral, 1977).

In the more general case of varying subsurface velocity, equation (32) becomes an approximation for diffraction traveltime that is routinely used in prestack time migration (Yilmaz, 2001). $\hat{T}$ then denotes the one-way traveltime of the image ray from the point scatter to the surface and the escape location x_0 of the image ray will

generally be different from the true location of the point scatterer in the Cartesian co-ordinates. The velocity v becomes time-migration velocity V_m, which will be selected for the best fit traveltime to equation (32).

To further understand equation (32) in heterogeneous media, we follow the derivation by **?** and consider the general one-way traveltime approximation centered around the image ray from the point scatterer to any surface point x given by,

$$t = \hat{T} + \frac{\hat{x}^2}{2} \left.\frac{\partial^2 t}{\partial \hat{x}^2}\right|_{\hat{x}=0} + \frac{\hat{x}^3}{6} \left.\frac{\partial^3 t}{\partial \hat{x}^3}\right|_{\hat{x}=0} + O(\hat{x}^4) \; , \tag{33}$$

where $\hat{x} = x - x_0$ denotes the distance between the escape location x_0 and any sur-rounding point x on the surface. Note that $\hat{x}$ functions similarly to h in equation (5) but has a different meaning than the conventional half offset when considering re-flection traveltime. The first-order term in equation (33) is always equal to zero due to the image rays always having zero phase slowness tangent to the surface, or equivalently to $\partial t/\partial \hat{x} = 0$ at $\hat{x} = 0$. We emphasize the notable presence of possible third-order term $(\hat{x}^3)$. This term can be neglected when $\hat{x}$ is sufficiently small or when the medium under consideration provides additional symmetry to the function of traveltime such as in homogeneous or horizontally layered VTI media, where trav-eltime varies as an even function around $\hat{x} = 0$. Converting equation (33) to a series in traveltime squared gives

$$t^2 = \hat{T}^2 + \hat{x}^2 \hat{T} \left.\frac{\partial^2 t}{\partial \hat{x}^2}\right|_{\hat{x}=0} + O(\hat{x}^3) \; . \tag{34}$$

Using equation (34), we can compute the total traveltime from a source at $m + h$ to point scatterer and to a receiver at $m - h$ as follows,

$$t_s + t_r = \sqrt{\hat{T}^2 + (m - h - x_0)^2 \hat{T} \left.\frac{\partial^2 t}{\partial \hat{x}^2}\right|_{\hat{x}=0}} + \sqrt{\hat{T}^2 + (m + h - x_0)^2 \hat{T} \left.\frac{\partial^2 t}{\partial \hat{x}^2}\right|_{\hat{x}=0}} + O(\hat{x}^3) \; . \tag{35}$$

Equation (35) suggests that equation (32) simply represents a sum of two Taylor expansions of the one-way traveltime from the point scatterer to the source and the receiver. Therefore, the migration velocity V_m can be related to the one-way traveltime derivatives as shown in equation (7). Moreover, our proposed framework to study the effects of weak lateral heterogeneity on one-way traveltime is applicable to v_m provided that the image ray is assumed to be sufficiently close to the vertical direction, which is exactly true in the case of 1D layered anisotropic media with horizontal symmetry planes.

APPENDIX B
DERIVATION OF THE RECURSIVE FORMULA

In this appendix, we provide a detailed derivation of the studied recursive formula (equation (12)) and discuss a possible extension to evaluate higher-order traveltime

derivatives. We start from the case of two-layer media previously investigated by Blias (1981), Blyas et al. (1984), Gritsenko (1984), and Goldin (1986) and proceed to the case of three-layered media to show how the recursion can be established for multi-layer media.

Two-layer case

Consider the two-layer setup shown in the left plot of Figure 15. In our notation, the total one-way traveltime is equal to

$$t = t_0(\mathbf{x_0}, \mathbf{x_1}(h)) + t_1(\mathbf{x_1}(h), \mathbf{x_2}(h)) \quad \text{where} \quad h = x_2 - x_0 \ . \tag{36}$$

By definition of $\mathbf{x}_k = \big(x_k, f_k(x_k)\big)$, we may write equation (36) as

$$t = t_0(x_0, x_1(h)) + t_1(x_1(h), x_2(h)) \quad \text{where} \quad h = x_2 - x_0 \ . \tag{37}$$

We emphasize the simple relationship between x_2 and h and differentiating equation (37) with respect to h to obtain

$$\frac{\partial t}{\partial h} = \frac{\partial t_1}{\partial h} + \frac{\partial t}{\partial x_1}\frac{dx_1}{dh} \ , \tag{38}$$

where the second term on the right-hand side disappear due to Fermat's principle ($\partial t/\partial x_1 = 0$). Therefore, we have

$$\frac{\partial t}{\partial h} = \frac{\partial t_1}{\partial h} \ . \tag{39}$$

Further differentiating equation (39) with respect to h leads to

$$\frac{\partial^2 t}{\partial h^2} = \frac{\partial^2 t_1}{\partial h^2} + \frac{\partial^2 t_1}{\partial x_1 \partial h}\left(\frac{dx_1}{dh}\right) \ . \tag{40}$$

To evaluate the derivative in equation (40), we need dx_1/dh, which can be found from differentiating the Fermat's condition ($\partial t/\partial x_1 = 0$) with respect to h. This leads to

$$\frac{\partial^2 t_1}{\partial x_1 \partial h} + \frac{\partial^2 t}{\partial x_1^2}\left(\frac{dx_1}{dh}\right) = 0 \ , \tag{41}$$

and therefore,

$$\frac{dx_1}{dh} = -\left(\frac{\partial^2 t_1}{\partial x_1 \partial h}\right)\bigg/\left(\frac{\partial^2 t}{\partial x_1^2}\right) = -\left(\frac{\partial^2 t_1}{\partial x_1 \partial h}\right)\bigg/\left(\frac{\partial^2 (t_0 + t_1)}{\partial x_1^2}\right) \ . \tag{42}$$

Substituting equation (42) into equation (40) leads to the final expression for the two-layer case studied by Blias (1981), Blyas et al. (1984), Gritsenko (1984), and Goldin (1986):

$$\frac{\partial^2 t}{\partial h^2} = \frac{\partial^2 t_1}{\partial h^2} - \left(\frac{\partial^2 t_1}{\partial x_1 \partial h}\right)^2\bigg/\left(\frac{\partial^2 (t_0 + t_1)}{\partial x_1^2}\right) \ , \tag{43}$$

which relates the second-order total traveltime derivative at the surface ($\partial^2 t/\partial h^2$) to that of the interface below ($\partial^2 t_1/\partial h^2$). All pertaining derivatives in equation (43) can be found from equation (15) in the main text that include the first-order effects from lateral heterogeneity.

Two-layered **Three-layered**
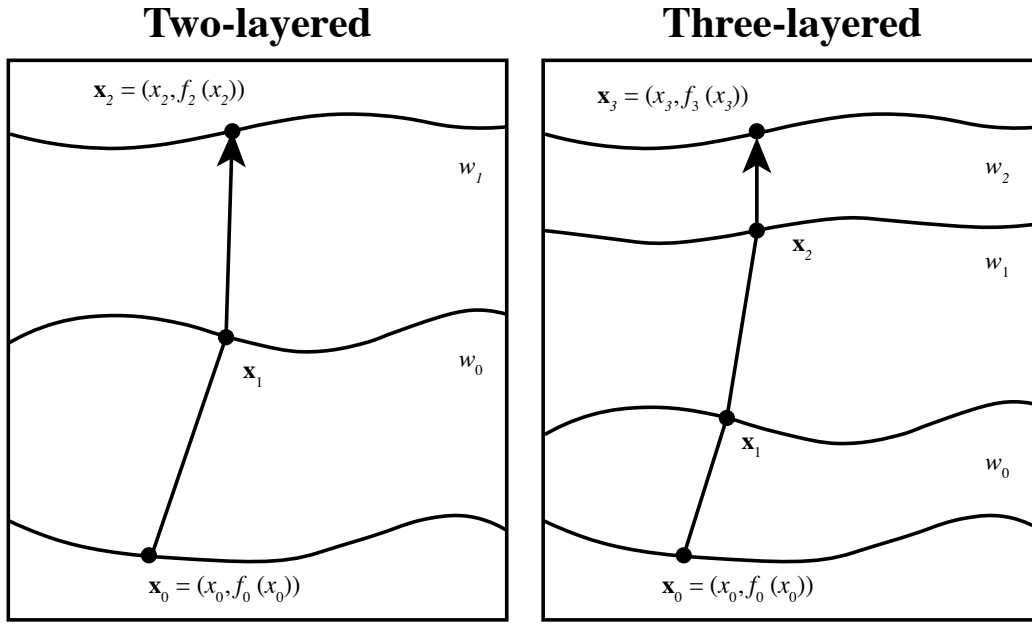
Figure 15: The ray configurations two- and three-layered media as the basis for relating the second-order traveltime derivatives at different interfaces.

Three-layer case

Let us now turn to the right plot of Figure 15, which depicts the situation where we have a three-layered medium and the total traveltime is given by

$$t = t_0(\mathbf{x_0}, \mathbf{x_1}(h)) + t_1(\mathbf{x_1}(h), \mathbf{x_2}(h)) + t_2(\mathbf{x_2}(h), \mathbf{x_3}(h)) \quad \text{where} \quad h = x_3 - x_0 . \quad (44)$$

We can proceed along the same line of argument as in the two-layer case and differentiating the total time with respect to h, which leads to

$$\frac{\partial t}{\partial h} = \frac{\partial t_2}{\partial h} + \sum_{k=1}^{2} \frac{\partial t}{\partial x_k} \frac{\partial x_k}{\partial h} . \quad (45)$$

Again, $\partial t/\partial x_k = 0$ due to the Fermat's principle, we then have

$$\frac{\partial t}{\partial h} = \frac{\partial t_2}{\partial h} . \quad (46)$$

We further differentiate the expression with respect to h and arrive at

$$\frac{\partial^2 t}{\partial h^2} = \frac{\partial^2 t_2}{\partial h^2} + \frac{\partial^2 t_2}{\partial x_2 \partial h} \left(\frac{dx_2}{dh} \right) . \quad (47)$$

To find dx_2/dh, we differentiate the Fermat's conditions ($\partial t/\partial x_k = 0$ for $k \in \{1, 2\}$) in a similar manner as in the two-layer case.

1. At the first interface ($k = 1$), the condition $\partial t/\partial x_1 = \partial(t_0 + t_1)/\partial x_1 = 0$ leads to

$$\frac{\partial^2(t_0 + t_1)}{\partial x_1^2}\left(\frac{dx_1}{dh}\right) + \frac{\partial^2 t_1}{\partial x_1 \partial x_2}\left(\frac{dx_2}{dh}\right) = 0 \tag{48}$$

2. At the second interface ($k = 2$), the condition $\partial t/\partial x_2 = \partial(t_1 + t_2)/\partial x_2 = 0$ leads to

$$\frac{\partial^2 t_1}{\partial x_1 \partial x_2}\left(\frac{dx_1}{dh}\right) + \frac{\partial^2(t_1 + t_2)}{\partial x_2^2}\left(\frac{dx_2}{dh}\right) + \frac{\partial^2 t_2}{\partial x_2 \partial h} = 0 \tag{49}$$

At this stage, we can see that equations (48) and (49) contain two unknown variables dx_1/dh and dx_2/dh to be solved for. We propose to look at this problem in a specific way that will facilitate an extension to the general multi-layer case. We first rearrange equation (48) into the following form

$$r = \left(\frac{dx_1}{dh}\right)\bigg/\left(\frac{dx_2}{dh}\right) = -\left(\frac{\partial^2 t_1}{\partial x_1 \partial x_2}\right)\bigg/\left(\frac{\partial^2(t_0 + t_1)}{\partial x_1^2}\right) , \tag{50}$$

which is reminiscent of equation (42) for the two-layer case when $x_2 = h + \text{const.}$ Substituting equation (50) into equation (49), we arrive at

$$\frac{dx_2}{dh} = -\left(\frac{\partial^2 t_2}{\partial x_2 \partial h}\right)\bigg/\left(r\frac{\partial^2 t_1}{\partial x_1 \partial x_2} + \frac{\partial^2(t_1 + t_2)}{\partial x_2^2}\right) , \tag{51}$$

which can be substituted into equation (47) to evaluate the desired second-order total traveltime derivative.

Multi-layer case

Looking closer at equations (48) and (49), we can observe that for each condition at the k-th interface, there are generally three terms:

$$\frac{\partial^2 t_{k-1}}{\partial x_{k-1} \partial x_k}\left(\frac{dx_{k-1}}{dh}\right) + \frac{\partial^2(t_{k-1} + t_k)}{\partial x_k^2}\left(\frac{dx_k}{dh}\right) + \frac{\partial^2 t_k}{\partial x_k \partial x_{k+1}}\left(\frac{dx_{k+1}}{dh}\right) = 0 , \tag{52}$$

where $k = 1, \ldots, n$ for a medium with $n + 1$ layers. The source at x_0 is fixed and therefore, $dx_0/dh = 0$. Moreover, the receiver is located at $x_{n+1} = h + x_0$, which leads to $dx_{n+1}/dh = 1$. Therefore, we can derive the following set of equations in the general case of multi-layer media:

$$\frac{\partial^2(t_0 + t_1)}{\partial x_1^2}\left(\frac{dx_1}{dh}\right) + \frac{\partial^2 t_1}{\partial x_1 \partial x_2}\left(\frac{dx_2}{dh}\right) = 0 , \tag{53}$$

$$\frac{\partial^2 t_1}{\partial x_1 \partial x_2}\left(\frac{dx_1}{dh}\right) + \frac{\partial^2(t_1 + t_2)}{\partial x_2^2}\left(\frac{dx_2}{dh}\right) + \frac{\partial^2 t_2}{\partial x_2 \partial x_3}\left(\frac{dx_3}{dh}\right) = 0 ,$$

$$\vdots$$

$$\frac{\partial^2 t_{n-1}}{\partial x_{n-1} \partial x_n}\left(\frac{dx_{n-1}}{dh}\right) + \frac{\partial^2(t_{n-1} + t_n)}{\partial x_n^2}\left(\frac{dx_n}{dh}\right) + \frac{\partial^2 t_n}{\partial x_n \partial h} = 0 ,$$

which leads to the recursive formula

$$r_k = \left(\frac{dx_k}{dh}\right)\bigg/\left(\frac{dx_{k+1}}{dh}\right) = -\left(\frac{\partial^2 t_k}{\partial x_k \partial x_{k+1}}\right)\bigg/\left(r_{k-1}\frac{\partial^2 t_{k-1}}{\partial x_{k-1}\partial x_k} + \frac{\partial^2 (t_{k-1}+t_k)}{\partial x_k^2}\right) \,, \tag{54}$$

where $r_0 = 0$ due to $dx_0/dh = 0$. This newly developed equation is an exact extension of the two-layer case result (equation (42)) to the multi-layer case and is similar to equation (12) in the main text.

APPENDIX C
A SUMMATION SCHEME TO ACCUMULATE HETEROGENEITY EFFECTS

As opposed to the exact recursion proposed in this study, a simpler summation scheme was previously used to accumulate the effects from heterogeneity. A review of this concept can be found in Blias (2006) and we briefly summarize the essentials here. One way to interpret this summation process is to examine one interface at a time and assume that apart from the considered interface, other intermediate layers between the source at larger depth and the receiver at the surface are laterally homogeneous (1D). Under this assumption, one can evaluate the contribution from lateral heterogeneity for this particular interface and its two adjacent layers using the result from the two-layer case (equation (43)). To further describe this process, we first assume that all sublayers are homogeneous isotropic similarly to what was done by Blias and consider only one non-flat interface at i-th. Therefore, we have

$$\frac{\partial^2 t}{\partial h^2} = \frac{\partial^2 \tau_i}{\partial h^2} - \left(\frac{\partial^2 \tau_i}{\partial x_i \partial h}\right)^2 \bigg/ \left(\frac{\partial^2(\tau_{i-1}+\tau_i)}{\partial x_i^2}\right) \,, \tag{55}$$

where $\tau_0 = \sum_{k=0}^{i-1} t_k$ and $\tau_1 = \sum_{k=i}^{n} t_k$ denote the effective time below and above the non-flat i-th interface. To evaluate pertaining derivatives, we use equation (15) for general media in the main text and focus only on the effects from curved interfaces at the moment by setting $W' = W'' = 0$ to exclude the effects from lateral velocity variations. Subsequently, we can derive the following expressions:

$$\frac{\partial^2 \tau_i}{\partial h^2}\bigg|_{h=0} = \frac{1}{\sum_{k=i}^{n} D_k/W_k} = \frac{1}{A} \,, \tag{56}$$

$$\frac{\partial^2 \tau_i}{\partial x_i \partial h}\bigg|_{h=0} = -\frac{1}{\sum_{k=i}^{n} D_k/W_k} = -\frac{1}{A} \,,$$

$$\frac{\partial^2 \tau_{i-1}}{\partial x_i^2}\bigg|_{h=0} = \frac{1}{\sum_{k=0}^{i-1} D_k/W_k} - F_i'' W_{i-1} = \frac{1}{B} - F_i'' W_{i-1} \,,$$

$$\frac{\partial^2 \tau_i}{\partial x_i^2}\bigg|_{h=0} = \frac{1}{\sum_{k=i}^{n} D_k/W_k} + F_i'' W_i = \frac{1}{A} + F_i'' W_i \,,$$

where W_k is the slowness for each isotropic sublayer k and D_k is its thickness. We also introduce dummy variables A and B to facilitate subsequent derivation. Substituting equation (56) into equation (55) leads to

$$\frac{\partial^2 t}{\partial h^2}\bigg|_{h=0} = \left(\frac{1}{A+B}\right) \left(\frac{1 + F_i''(W_i - W_{i-1})B}{1 + F_i''(W_i - W_{i-1})AB/(A+B)}\right) \qquad (57)$$

where $A + B = \sum_{k=0}^{n} D_k/W_k = TV_{rms}^2$ with T being the total one-way zero-offset traveltime in the 1D medium and V_{rms} being the corresponding root-mean-square velocity. Therefore, the first term on the right-hand side of equation (57) represents the usual second-order one-way traveltime derivative at zero offset in the 1D medium, whereas the second term is the contribution from lateral heterogeneity. When $F_i'' = 0$ for flat i-th interface, this second term becomes unity.

To further simplify equation (57), it can be linearized with respect to F'', which results in

$$\frac{\partial^2 t}{\partial h^2}\bigg|_{h=0} \approx \left(\frac{1}{A+B}\right) \left(1 + \frac{F_i''(W_i - W_{i-1})B^2}{A+B}\right) . \qquad (58)$$

Based on the result shown in equation (58), the total contribution from lateral heterogeneity due to various non-flat interfaces can be expressed as a summation on the term with F'' rather than being computed through a recursive evaluation as proposed in this study. Equation (58) is similar to equation 5 in Blias (2009b). For the effects from lateral velocity change (W''), a similar derivation procedure can be adopted. Finally, we emphasize that due to the steps taken in the derivation of equation (58), the terms involving $F'W'$ apparent in the general expressions in equation (15) are missing. These terms are also absent from the final result shown in equation 1 of Blias (2009b).

APPENDIX D
POSSIBLE EXTENSION TO HIGHER-ORDER DERIVATIVES

In this section, we discuss a possibility of extending our framework to evaluate higher-order one-way traveltime derivatives up to the fourth order. As reviewed in Appendix A, the fourth-order term is particularly important because it can be related to the quartic moveout coefficients for an estimation of anisotropy from reflection traveltime. Nonetheless, we emphasize the possible complications from reflection dispersal that may arise in the study of fourth-order traveltime derivatives for nonhyperbolic moveout (e.g., Pech et al., 2003).

Under similar assumptions used by equation (30), let us consider the two-layer model shown in the left plot of Figure 15 and differentiate the total traveltime

(equaiton (37)) with respect to h up to the fourth order, which gives

$$\frac{\partial t}{\partial h} = \frac{\partial t_1}{\partial h} + \frac{\partial t}{\partial x_1}\frac{dx_1}{dh} = \frac{\partial t_1}{\partial h} \, , \tag{59}$$

$$\frac{\partial^2 t}{\partial x_2^2} = \frac{\partial^2 t_1}{\partial h^2} + \boxed{\left(\frac{dx_1}{dh}\right)}\left(\frac{\partial^2 t_1}{\partial x_1 \partial h}\right) \, , \tag{60}$$

$$\frac{\partial^3 t}{\partial x_2^3} = \frac{\partial^3 t_1}{\partial h^3} + 2\boxed{\left(\frac{dx_1}{dh}\right)}\left(\frac{\partial^3 t_1}{\partial x_1 \partial h^2}\right) + \boxed{\left(\frac{dx_1}{dh}\right)^2}\left(\frac{\partial^3 t_1}{\partial x_1^2 \partial h}\right)$$

$$+ \boxed{\left(\frac{d^2 x_1}{dh^2}\right)}\left(\frac{\partial^2 t_1}{\partial x_1 \partial h}\right) \, , \tag{61}$$

$$\frac{\partial^4 t}{\partial x_2^4} = \frac{\partial^4 t_1}{\partial h^4} + 3\boxed{\left(\frac{dx_1}{dh}\right)}\left(\frac{\partial^4 t_1}{\partial x_1 \partial h^3}\right) + 3\boxed{\left(\frac{dx_1}{dh}\right)^2}\left(\frac{\partial^4 t_1}{\partial x_1^2 \partial h^2}\right)$$

$$+ 3\boxed{\left(\frac{dx_1}{dh}\right)\left(\frac{d^2 x_1}{dh^2}\right)}\left(\frac{\partial^3 t_1}{\partial x_1^2 \partial h}\right) + 3\boxed{\left(\frac{d^2 x_1}{dh^2}\right)}\left(\frac{\partial^3 t_1}{\partial x_1 \partial h^2}\right)$$

$$+ \boxed{\left(\frac{dx_1}{dh}\right)^3}\left(\frac{\partial^4 t_1}{\partial x_1^3 \partial h}\right) + \boxed{\left(\frac{d^3 x_1}{dh^3}\right)}\left(\frac{\partial^2 t_1}{\partial x_1 \partial h}\right) \, , \tag{62}$$

where we highlight the terms that have to be computed recursively for multi-layer media. These include additional second- $(d^2 x_1/dh^2)$ and third-order derivatives $(d^3 x_1/dh^3)$. In principle, one may therefore, with proper care, further differentiating the Fermat's conditions at different interfaces to obtain the required recursive formulas along the same line as what we did in the derivation of equation (54). An approximation in the same manner as Blias (2006) suitable for the second-order traveltime derivative mentioned in Appendix C may lead to more simplified and manageable expressions.

The one-way traveltime derivatives in each layer that include the effects of lateral heterogeneity can be straightforwardly computed using the current framework (equations (4), (13), and (14)) and we list them here for future references. We limit our consideration for the derivatives of F and W up to the second order in spatial derivatives. These following expressions must be used in conjunction with the exact or approximated recursive formulas that take into account higher-order terms to accumulate the effects of lateral heterogeneity from all layers on reflection or diffraction

traveltime. Parameters related to the third-order traveltime derivatives include

$$\left.\frac{\partial^3 t_k}{\partial x_k^3}\right|_{h=0} = \left.\frac{\partial^3 T_k}{\partial x_k^3}\right|_{h=0} + H_4 \ , \tag{63}$$

$$\left.\frac{\partial^3 t_k}{\partial x_k^2 \partial x_{k+1}}\right|_{h=0} = \left.\frac{\partial^3 T_k}{\partial x_k^2 \partial x_{k+1}}\right|_{h=0} + H_5 \ ,$$

$$\left.\frac{\partial^3 t_k}{\partial x_k \partial x_{k+1}^2}\right|_{h=0} = \left.\frac{\partial^3 T_k}{\partial x_k \partial x_{k+1}^2}\right|_{h=0} + H_6 \ ,$$

$$\left.\frac{\partial^3 t_k}{\partial x_{k+1}^3}\right|_{h=0} = \left.\frac{\partial^3 T_k}{\partial x_{k+1}^3}\right|_{h=0} + H_7 \ ,$$

where we use k as a dummy index and the heterogeneous terms are given by

$$H_4 = W_k'' F_k' + \frac{3W_k'}{2}\left(\frac{1}{F_k - F_{k+1}} + F_k''\right) - \frac{3W_k F_k'}{(F_k - F_{k+1})^2} \ , \tag{64}$$

$$H_5 = \frac{W_k''}{3}(F_k' - F_{k+1}') - \frac{W_k'}{2}\left(\frac{1}{F_k - F_{k+1}} - F_k''\right) + \frac{W_k(2F_k' + F_{k+1}')}{(F_k - F_{k+1})^2} \ ,$$

$$H_6 = \frac{W_k''}{3}(F_k' - F_{k+1}') - \frac{W_k'}{2}\left(\frac{1}{F_k - F_{k+1}} - F_{k+1}''\right) - \frac{W_k(F_k' + 2F_{k+1}')}{(F_k - F_{k+1})^2} \ ,$$

$$H_7 = -W_k'' F_{k+1}' + \frac{3W_k'}{2}\left(\frac{1}{F_k - F_{k+1}} - F_{k+1}''\right) + \frac{3W_k F_{k+1}'}{(F_k - F_{k+1})^2} \ .$$

Parameters related to the fourth-order traveltime derivatives include

$$\left.\frac{\partial^4 t_k}{\partial x_k^4}\right|_{h=0} = \left.\frac{\partial^4 T_k}{\partial x_k^4}\right|_{h=0} + H_8 \ , \tag{65}$$

$$\left.\frac{\partial^4 t_k}{\partial x_k^3 \partial x_{k+1}}\right|_{h=0} = \left.\frac{\partial^4 T_k}{\partial x_k^3 \partial x_{k+1}}\right|_{h=0} + H_9 \ ,$$

$$\left.\frac{\partial^4 t_k}{\partial x_k^2 \partial x_{k+1}^2}\right|_{h=0} = \left.\frac{\partial^4 T_k}{\partial x_k^2 \partial x_{k+1}^2}\right|_{h=0} + H_{10} \ ,$$

$$\left.\frac{\partial^4 t_k}{\partial x_k \partial x_{k+1}^3}\right|_{h=0} = \left.\frac{\partial^4 T_k}{\partial x_k \partial x_{k+1}^3}\right|_{h=0} + H_{11} \ ,$$

$$\left.\frac{\partial^4 t_k}{\partial x_{k+1}^4}\right|_{h=0} = \left.\frac{\partial^4 T_k}{\partial x_{k+1}^4}\right|_{h=0} + H_{12} \ ,$$

where the heterogeneous terms are given by

$$H_8 = 2W_k'' \left(\frac{1}{F_k - F_{k+1}} + F_k'' \right) - \frac{6W_k' F_k'}{(F_k - F_{k+1})^2} \tag{66}$$

$$- \frac{6W_k F_k''}{(F_k - F_{k+1})^2} + \frac{12W_k F_k'^2}{(F_k - F_{k+1})^3} \, ,$$

$$H_9 = -\frac{W_k''}{2} \left(\frac{1}{F_k - F_{k+1}} - F_k'' \right) + \frac{3W_k'(F_k' + F_{k+1}')}{2(F_k - F_{k+1})^2}$$

$$- \frac{6W_k F_k'(F_k' + F_{k+1}')}{(F_k - F_{k+1})^3} + \frac{3W_k F_k''}{(F_k - F_{k+1})^2} \, ,$$

$$H_{10} = \frac{W_k''(F_k'' - F_{k+1}'')}{3} + \frac{W_k'(F_k' - F_{k+1}')}{(F_k - F_{k+1})^2}$$

$$+ \frac{2W_k(F_k'^2 + 4F_k' F_{k+1}' + F_{k+1}'^2)}{(F_k - F_{k+1})^3} - \frac{W_k(F_k'' - F_{k+1}'')}{(F_k - F_{k+1})^2} \, ,$$

$$H_{11} = -\frac{W_k''}{2} \left(\frac{1}{F_k - F_{k+1}} + F_{k+1}'' \right) - \frac{3W_k'(F_k' + F_{k+1}')}{2(F_k - F_{k+1})^2}$$

$$- \frac{6W_k F_{k+1}'(F_k' + F_{k+1}')}{(F_k - F_{k+1})^3} - \frac{3W_k F_{k+1}''}{(F_k - F_{k+1})^2} \, ,$$

$$H_{12} = 2W_k'' \left(\frac{1}{F_k - F_{k+1}} - F_{k+1}'' \right) + \frac{6W_k' F_{k+1}'}{(F_k - F_{k+1})^2}$$

$$+ \frac{6W_k F_{k+1}''}{(F_k - F_{k+1})^2} + \frac{12W_k F_{k+1}'^2}{(F_k - F_{k+1})^3} \, .$$

APPENDIX E
POSSIBLE EXTENSION TO 3D

In this section, we discuss a possibility of extending the recursive formulation for 2D media in Appendix B to 3D media.

Two-layer case

Let us first consider the two-layer setup. In our notation, the total one-way traveltime in a 3D medium is equal to

$$t = t_0(x_0, y_0, x_1(h_x, h_y), y_1(h_x, h_y)) + t_1(x_1(h_x, h_y), y_1(h_x, h_y), x_2(h_x), y_2(h_y)) \, , \tag{67}$$

where $h_x = x_2 - x_0$ and $h_y = y_2 - y_0$. Equation (67) is the 3D version of equation (37). We can proceed along the same line as before and differentiate equation (67) to obtain

$$\frac{\partial^2 t}{\partial h_x^2} = \frac{\partial^2 t_1}{\partial h_x^2} + \frac{\partial^2 t_1}{\partial h_x \partial x_1} \frac{\partial x_1}{\partial h_x} + \frac{\partial^2 t_1}{\partial h_x \partial y_1} \frac{\partial y_1}{\partial h_x} \ , \tag{68}$$

$$\frac{\partial^2 t}{\partial h_y^2} = \frac{\partial^2 t_1}{\partial h_y^2} + \frac{\partial^2 t_1}{\partial h_y \partial x_1} \frac{\partial x_1}{\partial h_y} + \frac{\partial^2 t_1}{\partial h_y \partial y_1} \frac{\partial y_1}{\partial h_y} \ ,$$

$$\frac{\partial^2 t}{\partial h_x \partial h_y} = \frac{\partial^2 t_1}{\partial h_x \partial h_y} + \frac{\partial^2 t_1}{\partial h_x \partial x_1} \frac{\partial x_1}{\partial h_y} + \frac{\partial^2 t_1}{\partial h_x \partial y_1} \frac{\partial y_1}{\partial h_y} \ ,$$

$$= \frac{\partial^2 t_1}{\partial h_x \partial h_y} + \frac{\partial^2 t_1}{\partial h_y \partial x_1} \frac{\partial x_1}{\partial h_x} + \frac{\partial^2 t_1}{\partial h_y \partial y_1} \frac{\partial y_1}{\partial h_x} \ .$$

We can see from equation equation (68) that for 3D media, we need to find four derivatives (as opposed to only one in 2D media) in order to relate the traveltime derivatives from one surface to another. To find these four derivatives including $\partial x_1/\partial h_x$, $\partial x_1/\partial h_y$, $\partial y_1/\partial h_x$, and $\partial y_1/\partial h_y$, we differentiate the Fermat's condition for 3D medium:

$$\frac{\partial t}{\partial x_1} = \frac{\partial t}{\partial y_1} = 0 \ , \tag{69}$$

with respect to h_x and h_y, which leads to the following four conditions:

$$\frac{\partial^2 t}{\partial x_1^2} \frac{\partial x_1}{\partial h_x} + \frac{\partial^2 t}{\partial x_1 \partial y_1} \frac{\partial y_1}{\partial h_x} + \frac{\partial^2 t_1}{\partial x_1 \partial h_x} = 0 \ , \tag{70}$$

$$\frac{\partial^2 t}{\partial x_1^2} \frac{\partial x_1}{\partial h_y} + \frac{\partial^2 t}{\partial x_1 \partial y_1} \frac{\partial y_1}{\partial h_y} + \frac{\partial^2 t_1}{\partial x_1 \partial h_y} = 0 \ ,$$

$$\frac{\partial^2 t}{\partial x_1 \partial y_1} \frac{\partial x_1}{\partial h_x} + \frac{\partial^2 t}{\partial y_1^2} \frac{\partial y_1}{\partial h_x} + \frac{\partial^2 t_1}{\partial y_1 \partial h_x} = 0 \ ,$$

$$\frac{\partial^2 t}{\partial x_1 \partial y_1} \frac{\partial x_1}{\partial h_y} + \frac{\partial^2 t}{\partial y_1^2} \frac{\partial y_1}{\partial h_y} + \frac{\partial^2 t_1}{\partial y_1 \partial h_y} = 0 \ .$$

Equation (70) represents a linear system of four equations to be solved for four unknown derivatives: $\partial x_1/\partial h_x$, $\partial x_1/\partial h_y$, $\partial y_1/\partial h_x$, and $\partial y_1/\partial h_y$. This is different from equation (42) for the case of 2D media, where we do not need to solve an additional linear system.

Multi-layer case

Turning to the 3D multi-layer case with $n + 1$ layers, we have

$$\frac{\partial^2 t}{\partial h_x^2} = \frac{\partial^2 t_n}{\partial h_x^2} + \frac{\partial^2 t_n}{\partial h_x \partial x_n}\frac{\partial x_n}{\partial h_x} + \frac{\partial^2 t_n}{\partial h_x \partial y_n}\frac{\partial y_n}{\partial h_x} \ , \tag{71}$$

$$\frac{\partial^2 t}{\partial h_y^2} = \frac{\partial^2 t_n}{\partial h_y^2} + \frac{\partial^2 t_n}{\partial h_y \partial x_n}\frac{\partial x_n}{\partial h_y} + \frac{\partial^2 t_n}{\partial h_y \partial y_n}\frac{\partial y_n}{\partial h_y} \ ,$$

$$\frac{\partial^2 t}{\partial h_x \partial h_y} = \frac{\partial^2 t_n}{\partial h_x \partial h_y} + \frac{\partial^2 t_n}{\partial h_x \partial x_n}\frac{\partial x_n}{\partial h_y} + \frac{\partial^2 t_n}{\partial h_x \partial y_n}\frac{\partial y_n}{\partial h_y} \ ,$$

$$= \frac{\partial^2 t_n}{\partial h_x \partial h_y} + \frac{\partial^2 t_n}{\partial h_y \partial x_n}\frac{\partial x_n}{\partial h_x} + \frac{\partial^2 t_n}{\partial h_y \partial y_n}\frac{\partial y_n}{\partial h_x} \ ,$$

where we need to find $\partial x_n / \partial h_x$, $\partial x_n / \partial h_y$, $\partial y_n / \partial h_x$, and $\partial y_n / \partial h_y$ from differentiating the Fermat's principle similar to the previous 2D case. The general form of the linear system of equations at the k-th interface can be written as

$$0 = \frac{\partial^2 t_{k-1}}{\partial x_{k-1}\partial x_k}\left(\frac{\partial x_{k-1}}{\partial h_x}\right) + \frac{\partial^2 t_{k-1}}{\partial y_{k-1}\partial x_k}\left(\frac{\partial y_{k-1}}{\partial h_x}\right) + \tag{72}$$

$$\frac{\partial^2 (t_{k-1} + t_k)}{\partial x_k^2}\left(\frac{\partial x_k}{\partial h_x}\right) + \frac{\partial^2 (t_{k-1} + t_k)}{\partial x_k \partial y_k}\left(\frac{\partial y_k}{\partial h_x}\right) +$$

$$\frac{\partial^2 t_k}{\partial x_k \partial x_{k+1}}\left(\frac{\partial x_{k+1}}{\partial h_x}\right) + \frac{\partial^2 t_k}{\partial x_k \partial y_{k+1}}\left(\frac{\partial y_{k+1}}{\partial h_x}\right) \ ,$$

$$0 = \frac{\partial^2 t_{k-1}}{\partial x_{k-1}\partial x_k}\left(\frac{\partial x_{k-1}}{\partial h_y}\right) + \frac{\partial^2 t_{k-1}}{\partial y_{k-1}\partial x_k}\left(\frac{\partial y_{k-1}}{\partial h_y}\right) +$$

$$\frac{\partial^2 (t_{k-1} + t_k)}{\partial x_k^2}\left(\frac{\partial x_k}{\partial h_y}\right) + \frac{\partial^2 (t_{k-1} + t_k)}{\partial x_k \partial y_k}\left(\frac{\partial y_k}{\partial h_y}\right) +$$

$$\frac{\partial^2 t_k}{\partial x_k \partial x_{k+1}}\left(\frac{\partial x_{k+1}}{\partial h_y}\right) + \frac{\partial^2 t_k}{\partial x_k \partial y_{k+1}}\left(\frac{\partial y_{k+1}}{\partial h_y}\right) \ ,$$

$$0 = \frac{\partial^2 t_{k-1}}{\partial x_{k-1}\partial y_k}\left(\frac{\partial x_{k-1}}{\partial h_x}\right) + \frac{\partial^2 t_{k-1}}{\partial y_{k-1}\partial y_k}\left(\frac{\partial y_{k-1}}{\partial h_x}\right) +$$

$$\frac{\partial^2 (t_{k-1} + t_k)}{\partial x_k \partial y_k}\left(\frac{\partial x_k}{\partial h_x}\right) + \frac{\partial^2 (t_{k-1} + t_k)}{\partial y_k^2}\left(\frac{\partial y_k}{\partial h_x}\right) +$$

$$\frac{\partial^2 t_k}{\partial y_k \partial x_{k+1}}\left(\frac{\partial x_{k+1}}{\partial h_x}\right) + \frac{\partial^2 t_k}{\partial y_k \partial y_{k+1}}\left(\frac{\partial y_{k+1}}{\partial h_x}\right) \ ,$$

$$0 = \frac{\partial^2 t_{k-1}}{\partial x_{k-1}\partial y_k}\left(\frac{\partial x_{k-1}}{\partial h_y}\right) + \frac{\partial^2 t_{k-1}}{\partial y_{k-1}\partial y_k}\left(\frac{\partial y_{k-1}}{\partial h_y}\right) +$$

$$\frac{\partial^2 (t_{k-1} + t_k)}{\partial x_k \partial y_k}\left(\frac{\partial x_k}{\partial h_y}\right) + \frac{\partial^2 (t_{k-1} + t_k)}{\partial y_k^2}\left(\frac{\partial y_k}{\partial h_y}\right) +$$

$$\frac{\partial^2 t_k}{\partial y_k \partial x_{k+1}}\left(\frac{\partial x_{k+1}}{\partial h_y}\right) + \frac{\partial^2 t_k}{\partial y_k \partial y_{k+1}}\left(\frac{\partial y_{k+1}}{\partial h_y}\right) \ ,$$

where $k = 1, \ldots, n$ for a medium with $n+1$ layers. The source at (x_0, y_0) is fixed and therefore, $\partial x_0/\partial h_x = \partial x_0/\partial h_y = \partial y_0/\partial h_x = \partial y_0/\partial h_y = 0$. Moreover, the receiver is located at $(x_{n+1}, y_{n+1}) = (h_x+x_0, h_y+y_0)$, which leads to $\partial x_{n+1}/\partial h_x = \partial y_{n+1}/\partial h_y = 1$ and $\partial y_{n+1}/\partial h_x = \partial x_{n+1}/\partial h_y = 0$.

Looking closer at equation (72), we can see that at the first interface ($k = 1$), we have four equations with eight unknowns: $\partial x_1/\partial h_x$, $\partial x_1/\partial h_y$, $\partial y_1/\partial h_x$, $\partial y_1/\partial h_y$, $\partial x_2/\partial h_x$, $\partial x_2/\partial h_y$, $\partial y_2/\partial h_x$, and $\partial y_2/\partial h_y$, which is different from the two-layer case in equation (70) that only has four unknowns. In our previous consideration of 2D media (Appendix B), we show that this problem can be circumvented by considering the ratio r_k (equation (54)) and formulating a recursive formula. However, it is not immediately apparent how the same strategy can be applied to the system of equations (72) for the 3D media. Therefore, future investigations are required to properly handle this problem and come up with an efficient implementation scheme to analyze influences from lateral heterogeneity on time-processing parameters in 3D media. For example, we may choose to adopt the same strategy as in Appendix D that would allows us to rely on equation (70) and approximately sum individual contributions. Finally, we note that the pertaining one-way traveltime derivatives in each layer — another ingredient apart from the recursive formula— can simply be obtained by extending equations (4), (13), and (14) to 3D to also account for the y-direction.

REFERENCES

Al-Dajani, A., and I. Tsvankin, 1998, Non-hyperbolic reflection moveout for horizontal transverse isotropy: Geophysics, **63**, no. 5, 1738–1753.

Blias, E., 1981, Approximation for a CMP traveltime function for a stratified medium with curvilinear interfaces and variable bed velocities: Soviet Geology and Geophysics, **22**, no. 11, 123–131.

——, 2006, Some kinematic problems for layered media with shallow velocity anomalies: Russian Geology and Geophysics, **47**, no. 5, 587–603.

——, 2009a, Long-offset NMO approximatiosn for a layered VTI model: Model study: 79th Annual International Meeting Expanded Abstracts, Society of Exploration Geophysicists, 3745–3748.

——, 2009b, Stacking velocities in the presence of overburden velocity anomalies: Geophysical Prospecting, **57**, 323–341.

Blias, E., and S. Gritsenko, 2003, Stacking velocities for different offsets in the medium with laterally inhomogeneous layers: 73th Annual International Meeting Expanded Abstracts, Society of Exploration Geophysicists, 2160–2163.

Blias, E., and V. Khatchatran, 2003, Optimization approach to traveltime inversion for a medium with laterally inhomogeneous curvilinear layers: 73th Annual International Meeting Expanded Abstracts, Society of Exploration Geophysicists, 670–673.

Blyas, E., S. A. Gritsenko, and V. S. Chernjak, 1984, Time field derivatives in stratified media: Soviet Geology and Geophysics, **25**, no. 5, 75–81.

Buland, A., O. Kolbjørnsen, and A. J. Carter, 2011, Bayesian dix inversion: Geophysics, **76**, no. 2, R15–R22.

Cameron, M. K., S. B. Fomel, and J. A. Sethian, 2007, Seismic velocity estimation from time migration: Inverse Problems, **23**, 1329–1369.

Chernjak, V. S., and S. A. Gritsenko, 1979, Interpretation of effective common-depth-point parameters for a spatial system of homogeneous beds with curved boundaries: Soviet Geology and Geophysics, **20**, 91–98.

Claerbout, J., 1996, Basic Earth Imaging. (http://sepwww.stanford.edu/sep/prof/bei11.2010.pdf).

Fomel, S., 1994, Recurrent formulas for derivatives of a CDP travel-time curve: Russian Geology and Geophysics, **35**, no. 2, 118–126.

——, 2014, Transforming prestack seismic data by gardner continuation: 84th Annual International Meeting Expanded Abstracts, Society of Exploration Geophysicists, 4643–4649.

Fomel, S., and V. Grechka, 2001, Nonhyperbolic reflection moveout of P-waves: An overview and comparison of reasons, *in* CWP-372.

Fomel, S., E. Landa, and M. T. Taner, 2007, Poststack velocity analysis by separation and imaging of seismic diffractions: Geophysics, **72**, no. 6, U89–U94.

Fomel, S., and A. Stovas, 2010, Generalized nonhyperbolic moveout approximation: Geophysics, **75**, no. 2, U9–U18.

Goldin, S. V., 1986, Seismic Traveltime Inversion: Society of Exploration Geophysicists.

Grechka, V., A. Pech, and I. Tsvankin, 2002, P-wave stacking-velocity tomography

for VTI media: Geophysical Prospecting, **50**, 151–168.

Grechka, V., and I. Tsvankin, 1998, 3-D description of normal moveout in anisotropic inhomogeneous media: Geophysics, **63**, no. 3, 1079–1092.

——, 1999, 3-D moveout inversion in azimuthally anisotropic media with lateral velocity variation: Theory and a case study: Geophysics, **64**, no. 4, 1202–1218.

——, 2002, NMO velocity surfaces and Dix-type formulas in anisotropic heterogeneous media: Geophysics, **67**, 939–951.

Gritsenko, S. A., 1984, Time field derivatives: Soviet Geology and Geophysics, **25**, 103–109.

——, 2013, Imaging of Geological Sections and Velocity Estimation by Common Depth Point: VSEGEI Press. (in Russian).

Gritsenko, S. A., and V. S. Chernjak, 2001, Linearized traveltime inversion of reflections from the bottom of a layer with laterally variable interval velocity: Geofizika, 19–24.

Hubral, P., 1977, Time migration—some ray theoretical aspects: Geophysical Prospecting, **25**, 738–745.

——, 1983, Computing true amplitude reflections in a laterally inhomogeneous earth: Geophysics, **48**, 1051–1062.

Hubral, P., and T. Krey, 1980, Interval Velocities from Seismic Reflection Time Measurements: Society of Exploration Geophysicists.

Iversen, E., M. Tygel, B. Ursin, and M. V. de Hoop, 2012, Kinematic time migration and demigration of reflections in pre-stack seismic data: Geophys. J. Int., **189**, 1635–1666.

Jones, L. E. A., and H. F. Wang, 1981, Ultrasonic velocities in cretaceous shales from the williston basin: Geophysics, **46**, 288–297.

Koren, Z., and I. Ravve, 2006, Constrained Dix inversion: Geophysics, **71**, no. 6, R113–R130.

——, 2017, Normal moveout coefficients for horizontally layered triclinic media: Geophysics, **82**, no. 4, WA119–WA145.

Krey, T., 1976, Computation of interval velocities from common reflection point moveout times for n layers with arbitrary dips and curvatures in three dimensions when assuming small shot-geophone distances: Geophysical Prospecting, **24**, 91–111.

Li, S., and S. Fomel, 2015, A robust approach to time-to-depth conversion and interval velocity estimation from time migration in the presence of lateral velocity variations: Geophysical Prospecting, **63**, 315–337.

Lynn, W. S., and J. F. Claerbout, 1982, Velocity estimation in laterally varying media: Geophysics, **47**, no. 6, 884–897.

Pech, A., and I. Tsvankin, 2004, Quartic moveout coefficient for a dipping azimuthally anisotropic layer: Geophysics, **69**, no. 3, 699–707.

Pech, A., I. Tsvankin, and V. Grechka, 2003, Quartic moveout coefficient: 3D description and application to tilted TI media: Geophysics, **68**, no. 5, 1600–1610.

Reshef, M., and E. Landa, 2009, Post-stack velocity analysis in the dip-angle domain using diffractions: Geophysical Prospecting, **57**, no. 5, 811–821.

Schleicher, J., M. Tygel, and P. Hubral, 2007, Seismic True-Amplitude Imaging: Society of Exploration Geophysicists.

Sripanich, Y., and S. Fomel, 2014, Two-point seismic ray tracing in layered media useing bending: 84th Annual International Meeting Expanded Abstracts, Society of Exploration Geophysicists, 3371–3376.

——, 2015, On anelliptic approximations for qP velocities in TI and orthorhombic media: Geophysics, **80**, no. 5, C89–C105.

——, 2016, Theory of interval traveltime parameter estimation in layered anisotropic media: Geophysics, **81**, no. 5, C253–C263.

——, 2018, Fast time-to-depth conversion and interval velocity estimation in the case of weak lateral variations: Geophysics, **83**, no. 3, S227–S235.

Sripanich, Y., S. Fomel, A. Stovas, and Q. Hao, 2017, 3D generalized nonhyperboloidal moveout approximation: Geophysics, **82**, no. 2, C49–C59.

Takanashi, M., and I. Tsvankin, 2011, Correction for the influence of velocity lenses on nonhyperbolic moveout inversion for VTI media: Geophysics, **76**, no. 3, WA13–WA21.

——, 2012, Moveout analysis of wide-azimuth data in the presence of lateral velocity variation: Geophysics, **77**, no. 3, U49–U62.

Taner, M. T., and F. Koehler, 1969, Velocity spectra – Digital computer derivation and applications of velocity functions: Geophysics, **34**, 859–881.

Thomsen, L., 2014, Understanding Seismic Anisotropy in Exploration and Exploitation, 2 ed.: Society of Exploration Geophysicists and European Association of Geoscientists and Engineers.

Tsvankin, I., 2012, Seismic Signatures and Analysis of Reflection Data in Anisotropic Media: Society of Exploration Geophysicists.

Tsvankin, I., and V. Grechka, 2011, Seismology of Azimuthally Anisotropic Media and Seismic Fracture Characterization: Society of Exploration Geophysicists.

Ursin, B., and A. Stovas, 2006, Traveltime approximations for a layered transversely isotropic medium: Geophysics, **71**, no. 2, D23–D33.

Valente, L. S., H. B. Santos, J. C. Costa, and J. Schleicher, 2017, Time-to-depth conversion and velocity estimation by image-wavefront propagation: Geophysics, **82**, no. 6, U75–U85.

Vernik, L., and X. Liu, 1997, Velocity anisotropy in shales: A petrophysical study: Geophysics, **62**, 521–532.

Wang, Z., 2002, Seismic anisotropy in sedimentary rocks, Part 2: Laboratory data: Geophysics, **67**, 1423–1440.

Yilmaz, O., 2001, Seismic data analysis, 2 ed.: Society of Exploration Geophysicists.